

N O T I C E

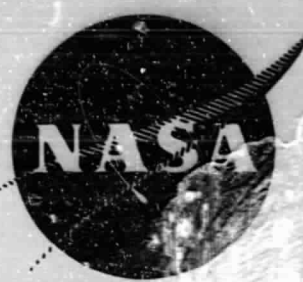
THIS DOCUMENT HAS BEEN REPRODUCED FROM
MICROFICHE. ALTHOUGH IT IS RECOGNIZED THAT
CERTAIN PORTIONS ARE ILLEGIBLE, IT IS BEING RELEASED
IN THE INTEREST OF MAKING AVAILABLE AS MUCH
INFORMATION AS POSSIBLE

NT
files

FK

2/78

R-0 3-78
NASA CR-135160 5-78
R75AEG511 6-78



QUIET CLEAN SHORT-HAUL EXPERIMENTAL ENGINE
(QCSEE)
CORE ENGINE NOISE MEASUREMENTS

by
H.D. Sowers
and
W.E. Coward

GENERAL ELECTRIC COMPANY

(NASA-CR-135160) QUIET CLEAN SHORT-HAUL
EXPERIMENTAL ENGINE (QCSEE). CORE ENGINE
NOISE MEASUREMENTS (General Electric Co.)
52 p HC A04/MF A01 CSCL 21E N80-15093
G3/07 Unclas 33470

prepared for

NATIONAL AERONAUTICS AND SPACE ADMINISTRATION



TABLE OF CONTENTS

<u>Section</u>		<u>Page</u>
I.	SUMMARY	1
II.	INTRODUCTION	2
III.	TEST SETUP	3
	A. F101 Engine Description	3
	B. Test Site and Instrumentation	3
	C. Test Conditions	9
IV.	TEST RESULTS AND ANALYSIS	10
	A. Farfield Data	10
	1. Ground Reflection Corrections	10
	2. Data Analysis	10
	B. Acoustic Probe Data	18
V.	CONCLUSIONS	45
VI.	REFERENCE	46

PRECEDING PAGE BLANK NOT FILMED

LIST OF ILLUSTRATIONS

<u>Figure</u>		<u>Page</u>
1.	Schematic of Engine Configuration.	4
2.	Schematic of Acoustic Test Facility.	5
3.	Test Site.	6
4.	Engine Test Stand.	7
5.	Acoustic Probe.	8
6.	Comparison of 40-ft and 1-ft Height Microphone Spectra.	11
7.	Comparison of Predicted and Measured Farfield Spectra, 41% Fan Speed.	12
8.	Comparison of Predicted and Measured Farfield Spectra, 54% Fan Speed.	13
9.	Comparison of Predicted and Measured Farfield Spectra, 67% Fan Speed.	14
10.	Comparison of Predicted and Measured Farfield Spectra, 80% Fan Speed.	15
11.	Comparison of Predicted and Measured Farfield Spectra, 93% Fan Speed.	16
12.	400 Hz 1/3-Octave Band SPL Versus Jet Velocity.	19
13.	400 Hz 1/3-Octave Band SPL Directivity, 41% Fan Speed.	20
14.	400 Hz 1/3-Octave Band SPL Directivity, 54% Fan Speed.	21
15.	400 Hz 1/3-Octave Band SPL Directivity, 67% Fan Speed.	22
16.	400 Hz 1/3-Octave Band SPL Directivity, 80% Fan Speed.	23
17.	400 Hz 1/3-Octave Band SPL Directivity, 93% Fan Speed.	24

LIST OF ILLUSTRATIONS (Continued)

<u>Figure</u>		<u>Page</u>
18.	630 Hz 1/3-Octave Band SPL Versus Jet Velocity.	25
19.	630 Hz 1/3-Octave Band SPL Directivity, 41% Fan Speed.	26
20.	630 Hz 1/3-Octave Band SPL Directivity, 54% Fan Speed.	27
21.	630 Hz 1/3-Octave Band SPL Directivity, 67% Fan Speed.	28
22.	630 Hz 1/3-Octave Band SPL Directivity, 80% Fan Speed.	29
23.	630 Hz 1/3-Octave Band SPL Directivity, 93% Fan Speed.	30
24.	Core Probe PWL Spectrum, 22% Fan Speed.	31
25.	Core Probe PWL Spectrum, 32% Fan Speed.	32
26.	Core Probe PWL Spectrum, 41% Fan Speed.	33
27.	Core Probe PWL Spectrum, 53% Fan Speed.	34
28.	Core Probe PWL Spectrum, 64% Fan Speed.	35
29.	Core Probe Narrowband SPL Spectrum, 22% Fan Speed.	37
30.	Core Probe Narrowband SPL Spectrum, 32% Fan Speed.	38
31.	Core Probe Narrowband SPL Spectrum, 41% Fan Speed.	39
32.	Core Probe Narrowband SPL Spectrum, 53% Fan Speed.	40
33.	Core Probe Narrowband SPL Spectrum, 64% Fan Speed.	41
34.	Probe Measured 1/3-Octave Band PWL Versus $20 \log (K)$.	42
35.	Low Pressure Turbine Stage 2 Fundamental PWL Versus Turbine Pressure Ratio.	44

SECTION I

SUMMARY

Farfield and nearfield acoustic measurements were taken on an F101 turbofan engine, in order to determine the core engine internally generated noise levels. The measured noise levels were then compared to the predicted core internal noise levels, employing the same prediction procedures used for the Quiet Clean Short-Haul Experimental Engine (QCSEE) system noise.

The farfield data with an involved analysis to define the core internal noise showed that the predicted levels do not vary significantly from the measured data. The nearfield (acoustic probe) measured levels are considerably higher than predicted. Two possible reasons for the differences are 1) inaccuracies in the prediction procedure for levels within the engine and 2) extraneous or psuedo noise signals recorded by the probes.

From the results it was concluded that no adjustments to the present farfield core internal noise predictions or suppressor design for the QCSEE engines were justified.

SECTION II

INTRODUCTION

It has already been well documented that internally generated noise from the engine core is becoming an increasingly important noise source in today's high bypass turbofan engines. In the case of the QCSEE engines, with their low jet and fan noise levels, and with the associated low system noise goals, the core internal noise is definitely a factor of importance. The system noise level predictions for both QCSEE engines indicate that acoustic suppression must be applied to the combustor and turbine noise if the sideline noise goals of 95 EPNdB are to be met. The methods used to predict the combustor and turbine noise for the QCSEE engine are semi-empirical correlations developed by General Electric during the Core Engine Noise Control Program (Reference 1). The accuracy of these prediction procedures has been established by comparisons with data from several engines. It is, however, difficult to ascertain the exact core noise levels from measured engine data, since these levels are still lower than other "extraneous" noise sources such as the fan and jet; for this reason, there are still some uncertainties regarding core noise predictions.

The ideal method to determine the accuracy of any noise prediction is, of course, to compare it with actual acoustic measurements from the engine or components to be employed in the system in question. Such an opportunity arose for the QCSEE core engine when an F101 engine test was scheduled for the GE test facility at Peebles, Ohio, in November of 1974. The QCSEE engines employ the same core engine as the F101 engine, with only minor changes being made to the low pressure turbine guide vanes.

The F101 Tests were to be conducted on the test stand normally employed for full-scale engine acoustic tests, so sound measurement facilities were readily available. The engine test configuration was acoustically unsuppressed, however, which meant that the core noise levels would be well below the fan and jet noise levels at all but the very lowest power settings.

Irrespective of this problem, it was felt that this test provided an opportunity to measure core internal noise on a "QCSEE-type" core engine. A series of low-power runs was requested to allow the recording of farfield acoustic data. Slight modifications were made to the engine to acoustically "clean up" the nozzle (removal of afterburner spraybars and flameholders). It was also determined that acoustic measurements would be made in the core duct, just downstream of the turbine exit, using a waveguide acoustic probe. These probes have an inherent disadvantage in that they record the aerodynamic pressure fluctuations, or "psuedonoise" as well as the actual acoustic signal in the duct (this tends to "mask" the broadband noise). They did, however, provide the only opportunity for measuring core noise in the duct.

The resulting acoustic tests were completed during the period of November 19th through November 22nd, 1974. The recording, reduction, and analysis of that test data is the subject of this report.

SECTION III

TEST SETUP

A. F101 Engine Description

The F101 engine is an augmented turbofan engine, with a two-stage fan driven by a two-stage low pressure turbine. The compressor is driven by a single-stage high pressure turbine. The exhaust is a mixed-flow configuration, with a multilobed "forced" mixer combining the fan and core flows. The exhaust nozzle is a variable area convergent-divergent device. The augmentor spraybars and flameholders are combined with the mixer, but for this test the spraybars and flameholders were removed to prevent extraneous noise generation. The test engine is shown schematically in Figure 1.

The core for the QCSEE engines is different in that the low pressure turbine exit guide vanes are modified and the "daisy" forced mixer on the core nozzle is eliminated.

B. Test Site and Instrumentation

The engine was installed on the acoustic test stand at the Peebles Test Facility. However, there were some obstructions in the sound field as a result of other tests being conducted on the engine.

The farfield microphone setup is shown in Figure 2. Due to the presence of the other equipment, no data were recorded from the microphones forward of 50°; also, some of the remaining microphones forward of 70° may be affected by the presence of obstructions. It was felt that this was not an undue hindrance, since the forward arc noise would almost certainly be dominated by unsuppressed fan noise. The "normal" microphone setup is at 45.7 m (150 ft) radius, employing microphones mounted at 12.2 m (40 ft) above the ground; this results in the ground "nulls" being shifted to the lower frequencies. Since this low frequency region is of primary interest in the measurement of core noise, it was decided to add a second arc of microphones which have the ground nulls at high frequency and thus to be used for evaluating low frequency noise. The second array of microphones was placed at a height of 0.305 m (1 ft) above the ground, over the center of a plywood surface 1.8 m x 1.8 m (6 ft x 6 ft). The microphones were mounted directly in front of the 12.2 m (40 ft) high microphones, resulting in a measurement arc distance of 43.9 m (144 ft). Figures 3 and 4 are photographs of the test site showing the relative positions of all items.

Location of the internal acoustic instrumentation is shown schematically in Figure 1. A noncooled waveguide acoustic probe, Figure 5, was used to traverse the core exhaust just downstream of the low pressure turbine exit guide vanes, access being gained through a hole normally occupied by an augmentor spraybar.

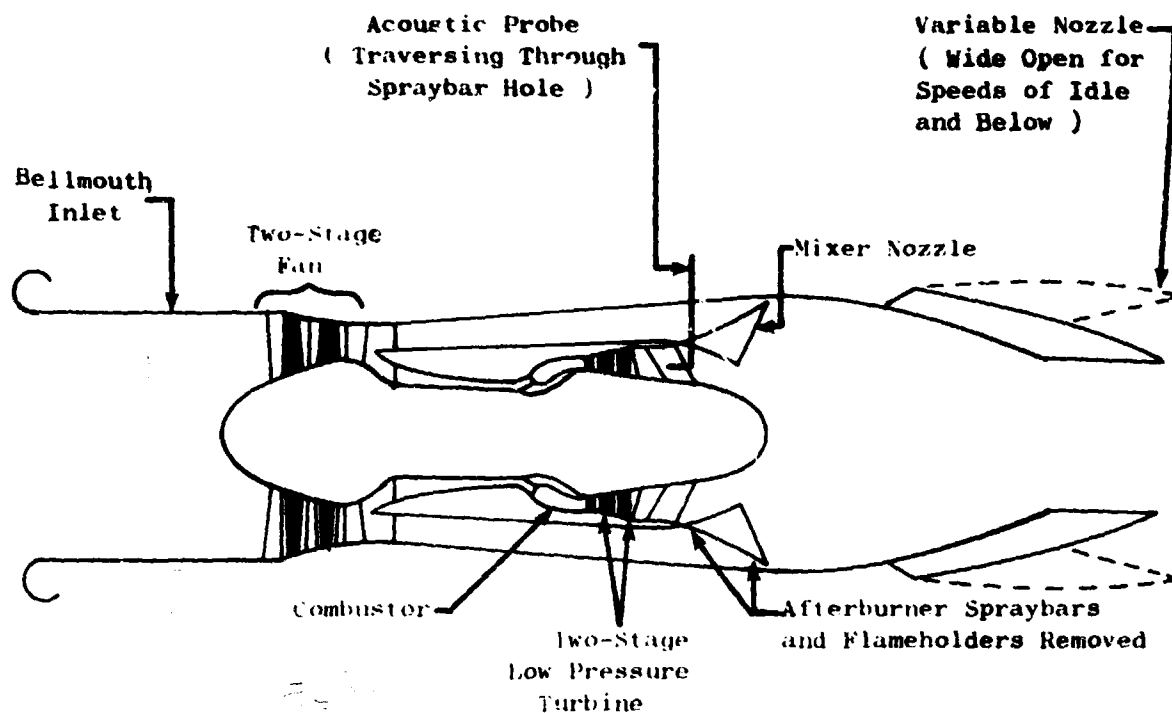
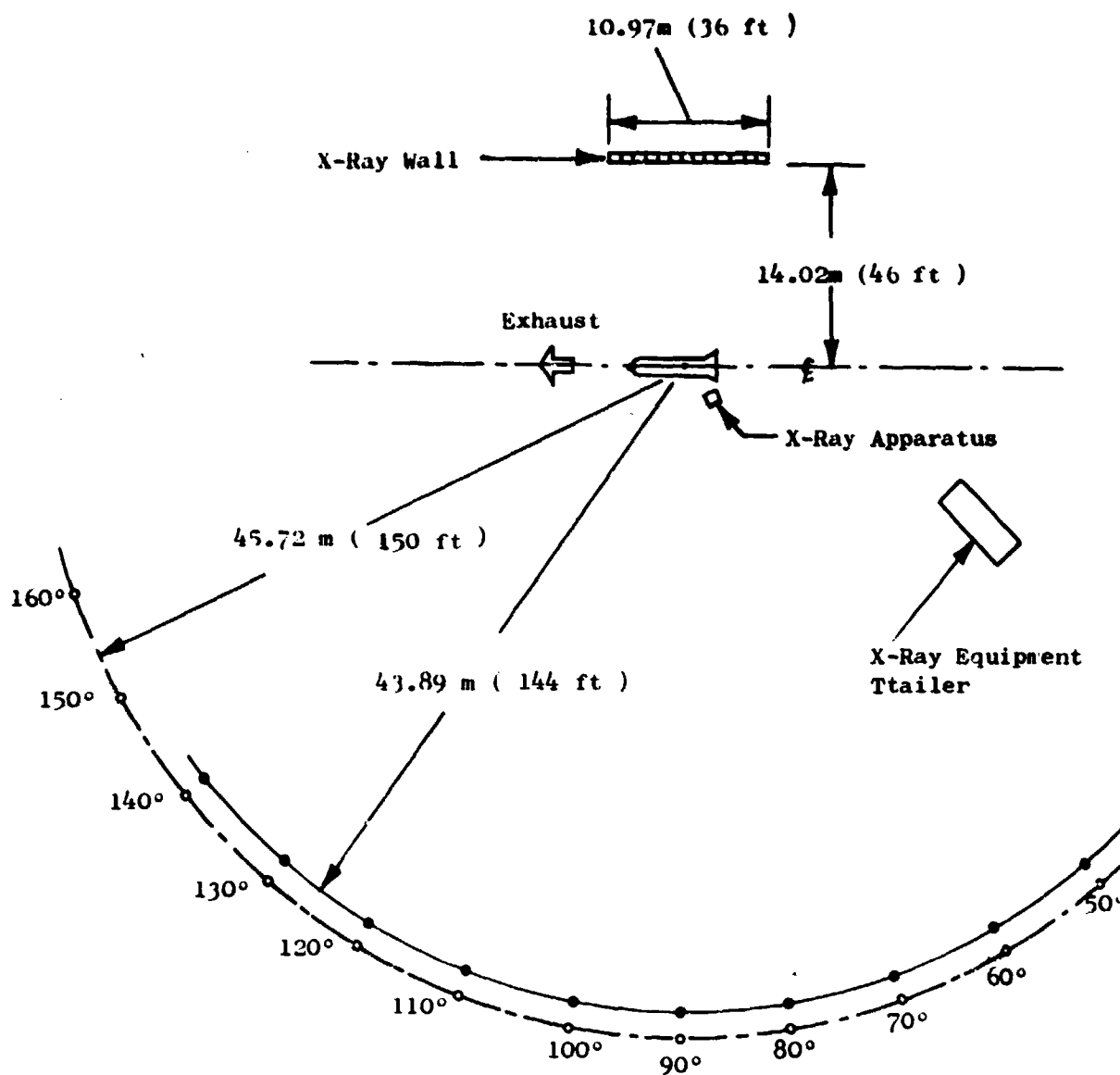


Figure 1. Schematic of Engine Configuration.



- 12.19 m (40 ft) Height Microphones
- 0.305 m (1 ft) Height Microphones
(Mounted over Plywood Surface)

Figure 2. Schematic of Acoustic Test Facility.

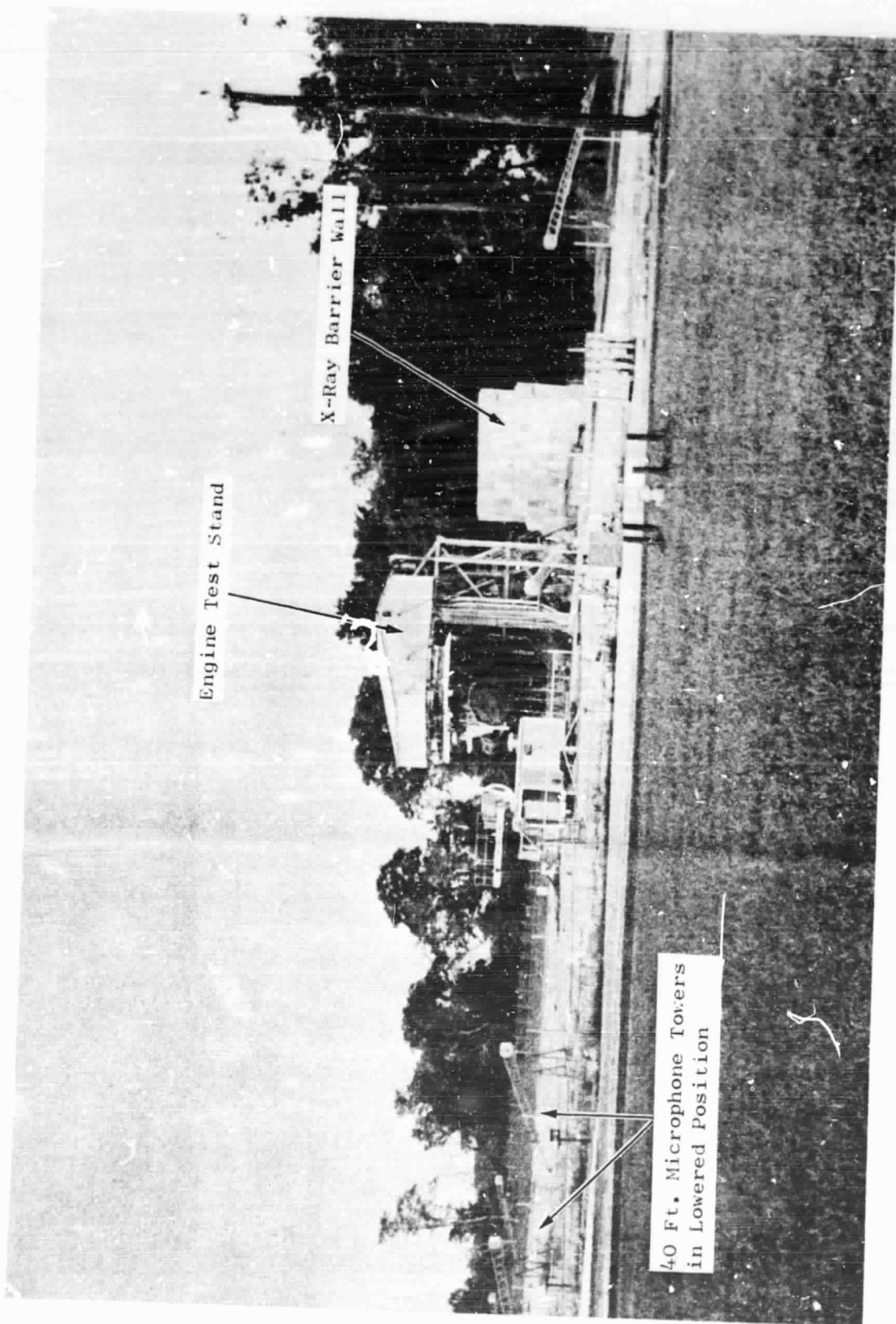


Figure 3. Test Site.

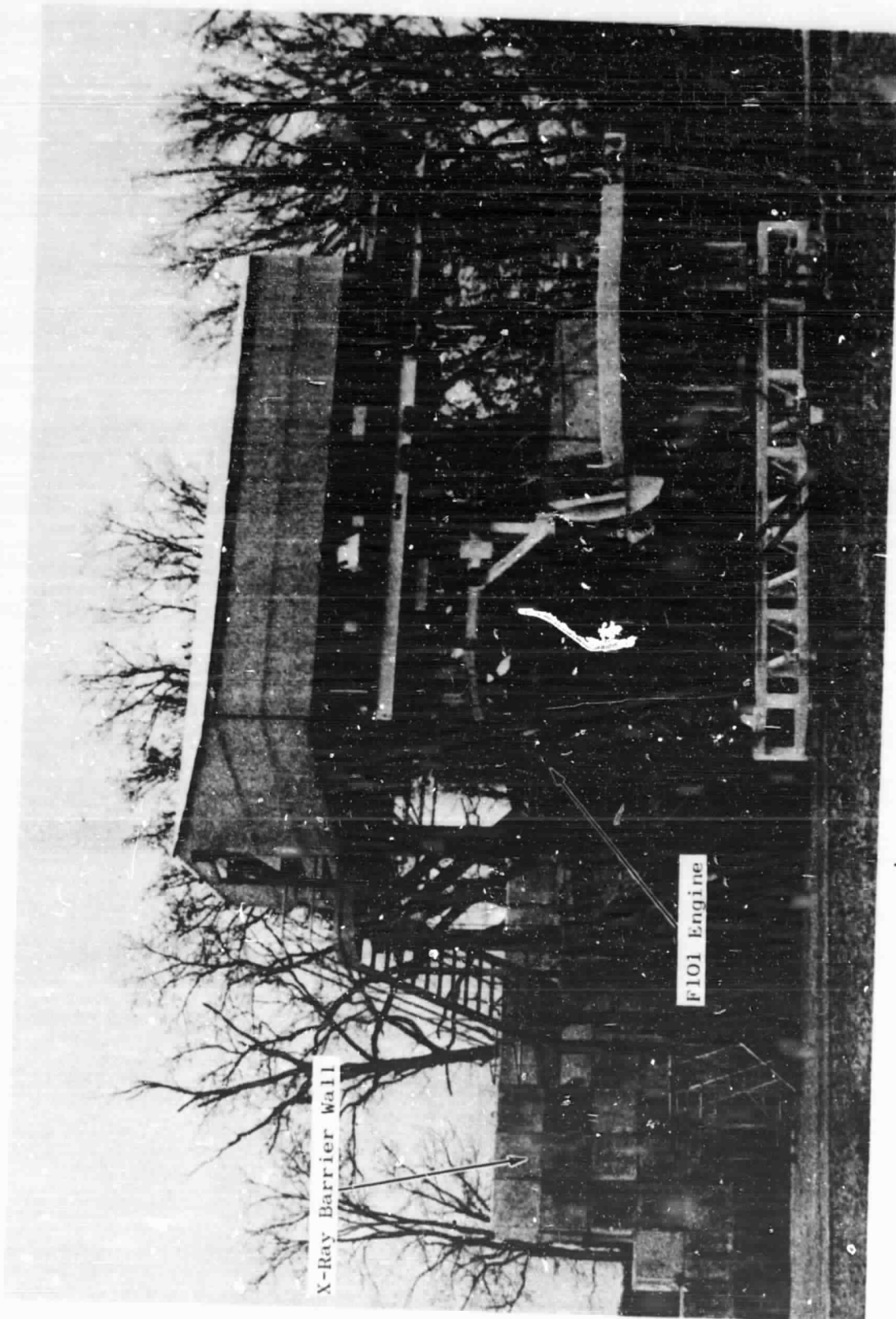


Figure 4. Engine Test Stand.

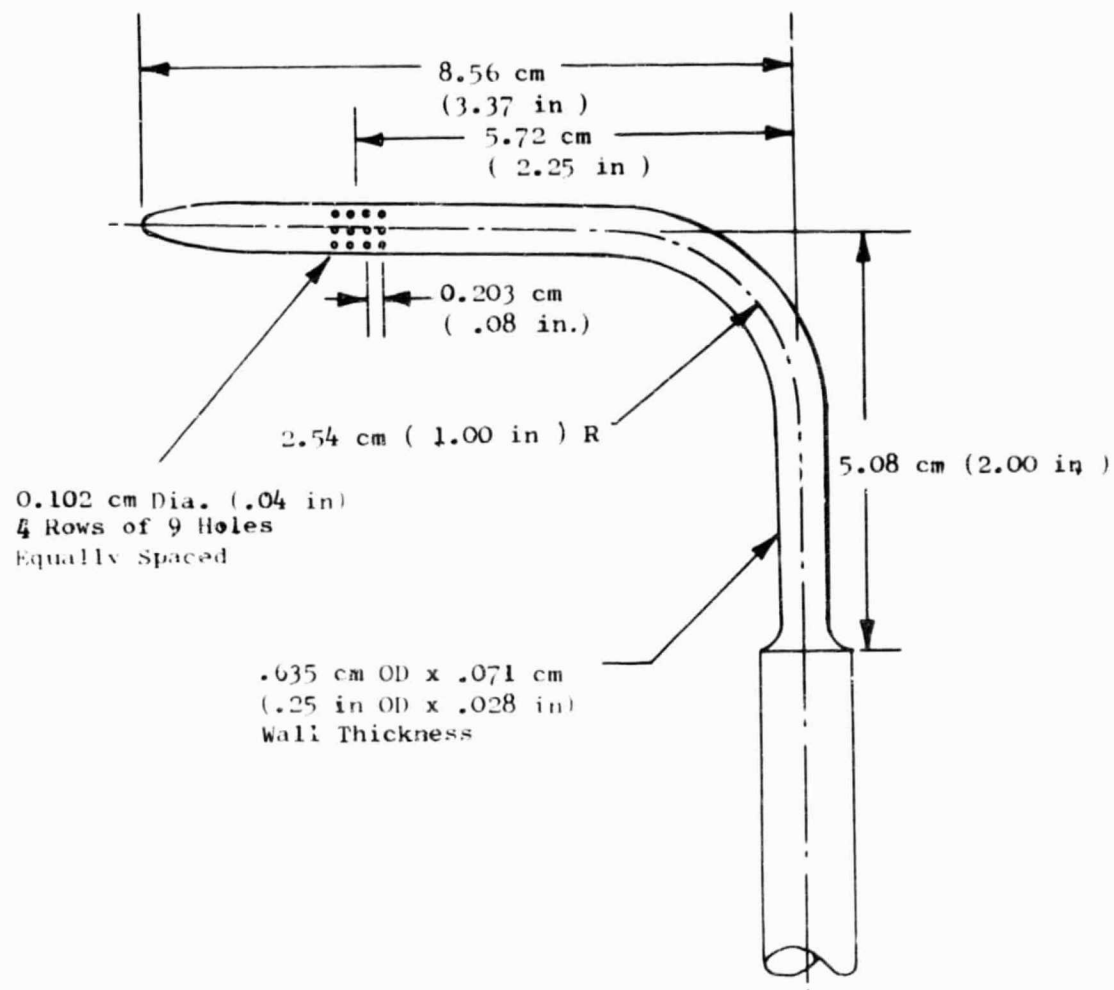


Figure 5. Acoustic Probe.

The aerodynamic instrumentation was limited to the necessary "safety" items. Rotational speeds, inlet temperature and pressure, and the turbine exhaust temperature were measured.

C. Test Conditions

As has been noted, there was no acoustic suppression on the engine. This meant that all high frequency farfield noise measurements would be heavily dominated by the fan noise. It was thought, however, that the low frequency fan noise would not interfere with the core noise measurements, particularly at the lower engine power settings where core noise could be detected in the farfield. The acoustic probe traverse was taken well up into the core duct, so fan noise was not expected to be of any significance for the probe data.

The low frequency farfield noise levels would, of course, be jet-noise dominated at the higher engine power settings, even for unaugmented operation. The acoustic measurements were thus made for a range of power settings that extended down to subidle power. The variable nozzle of the engine is at its "wide-open" position at and below idle power setting (41% fan speed). As speed is increased above idle, the nozzle rapidly starts to close down; thus there is a rapid fall-off in jet velocity as the power setting drops to idle.

Probe data were taken for fan speeds of 22%, 32%, 41%, 53%, and 64% of the maximum fan speed. Farfield acoustic data were recorded for fan speeds of 41%, 54%, 67%, 80% and 93%. Due to time limitations, farfield data points below idle (41% N_f) could not be obtained. Since the jet exhaust velocity is already very low at the idle power setting (approximately 65.5 m/sec (215 ft/sec), the loss of the subidle points was not thought to be important.

All acoustic data were recorded on magnetic tape for later reduction to one-third octave band format. The aerodynamic measurements were used, along with status cycle deck data, to estimate the internal conditions of flow through the fan, combustor, low pressure turbine, and exhaust nozzle for each acoustic test point. These estimated conditions were employed as inputs to the noise prediction procedures.

SECTION IV
TEST RESULTS AND ANALYSIS

A. Farfield Data

1. Ground Reflection Corrections

Two sets of farfield data were available, the 12.2 m (40 ft) height and 0.305 m (1 ft) height microphones. The 0.305 m (1 ft) height microphones were selected to obtain data at frequencies from 50 Hz through 320 Hz. In this frequency range these microphones would be expected to have data which is free of ground nulls and could be corrected for reinforcement below the first ground null. Ideally the first null would appear at 3200 Hz, however, due to the imperfect ground plane and the large incidence angle of the reflected wave, the first null occurs as low as 630 Hz as indicated on Figure 6. With the first null at this frequency the 50 to 320 Hz levels will still have some level of reinforcement. From analysis of the data it was concluded that a reinforcement correction of 2 dB would be representative over that frequency range. Thus all of the measured 0.305 m (1 ft) microphone data from 50 Hz through 320 Hz were reduced by 2 dB.

The height of the 12.2 m (40 ft) microphones was selected to give a ground reflection first null at 80 Hz. From the data of Figure 6 it can be seen that this null does occur as predicted. The smaller incidence angle of the reflected waves for these microphones is believed to be the reason for the better agreement between measured and predicted values. With the first null at 80 Hz the levels from 400 Hz and above were believed to be relatively free of ground effects, thus the 12.2 m (40 ft) microphone data were used at these frequencies.

2. Data Analysis

The one-third octave band spectra recorded in the farfield at the predicted maximum angle for combustor noise (120°) are shown in Figures 7 through 11. The data are compared to the predicted spectra for combustor, jet, and fan noise at the 45.7 m (150 ft) arc distance for all five power settings. The combustor noise prediction used is the same one employed for the QCSEE engine system status noise predictions. The predicted jet noise levels are based on scale model tests of a hot, dual-flow forced mixer nozzle of a configuration similar to the F101 nozzle. For the purposes of these comparisons, at low power settings, the noise levels above 1000 Hz were assumed to be fan noise; below 1000 Hz, the fan noise was assumed to ramp off at the rate of 2 dB per one-third octave band. This drop-off rate is based on the observation of noise data from several scale model fan tests.

- 120° Acoustic Angle
- 41% Fan Speed
- 45.72 m (150 ft) Arc

- 12.19 m (40 ft) Height Mics
- .305 m (1 ft) Height Mics

Solid Symbols Indicate Ground
Effects First Null

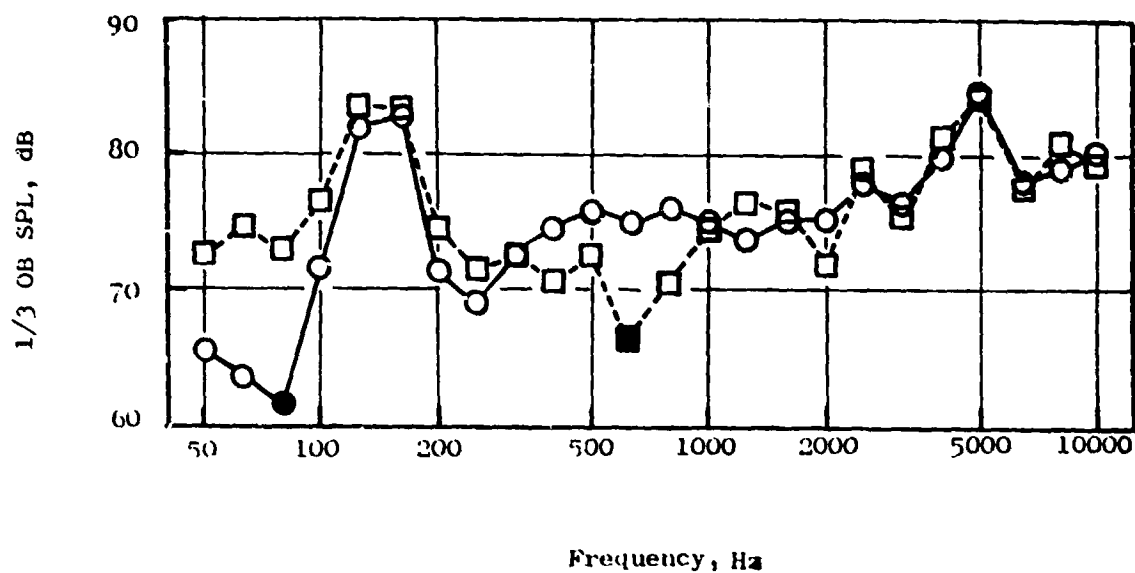


Figure 6. Comparison of 40-ft and 1-ft Height Microphone Spectra.

- 120° Acoustic Angle
- 41 % Fan Speed
- 45.72 m (150 ft) Arc

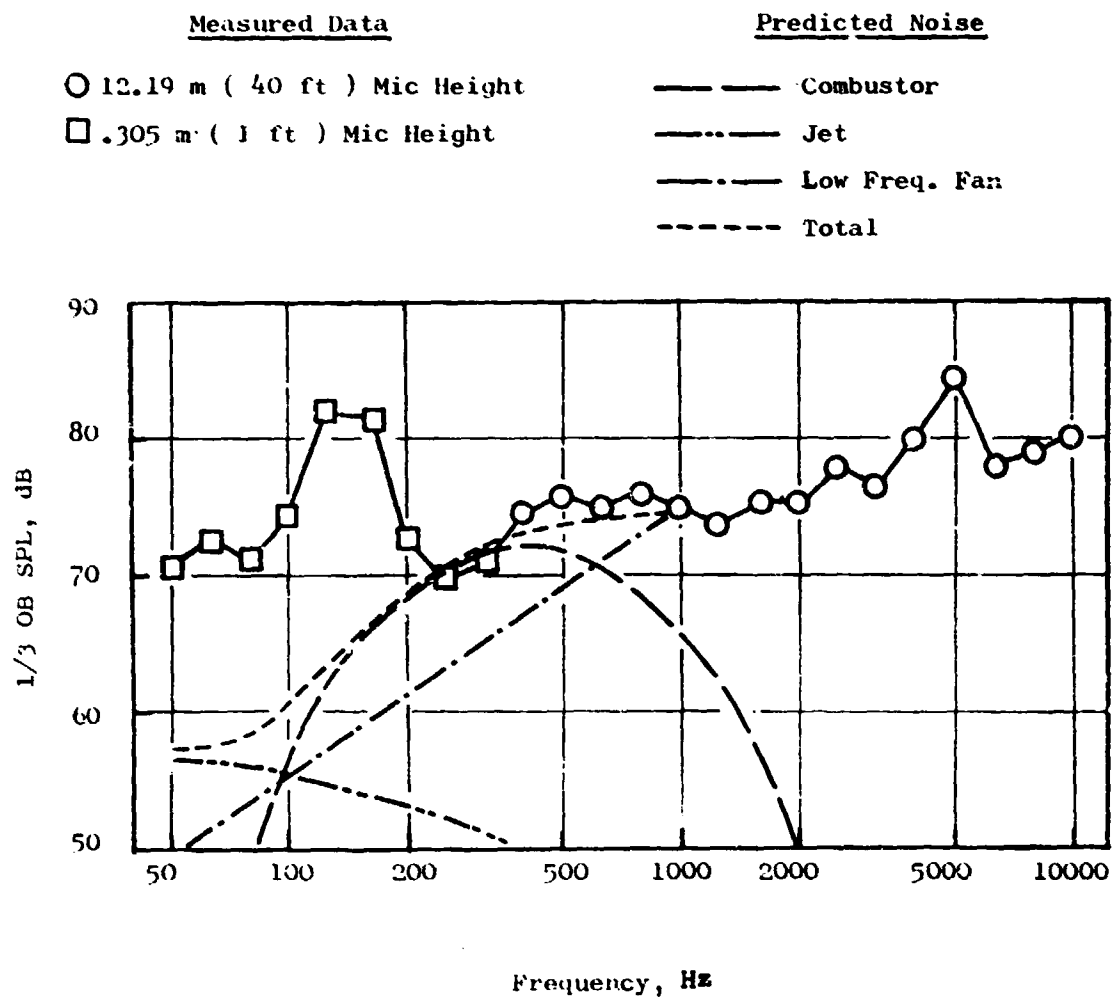


Figure 7. Comparison of Predicted and Measured Farfield Spectra, 41% Fan Speed.

- 120° Acoustic Angle
- 54% Fan Speed
- 45.72 m (150 ft) Arc

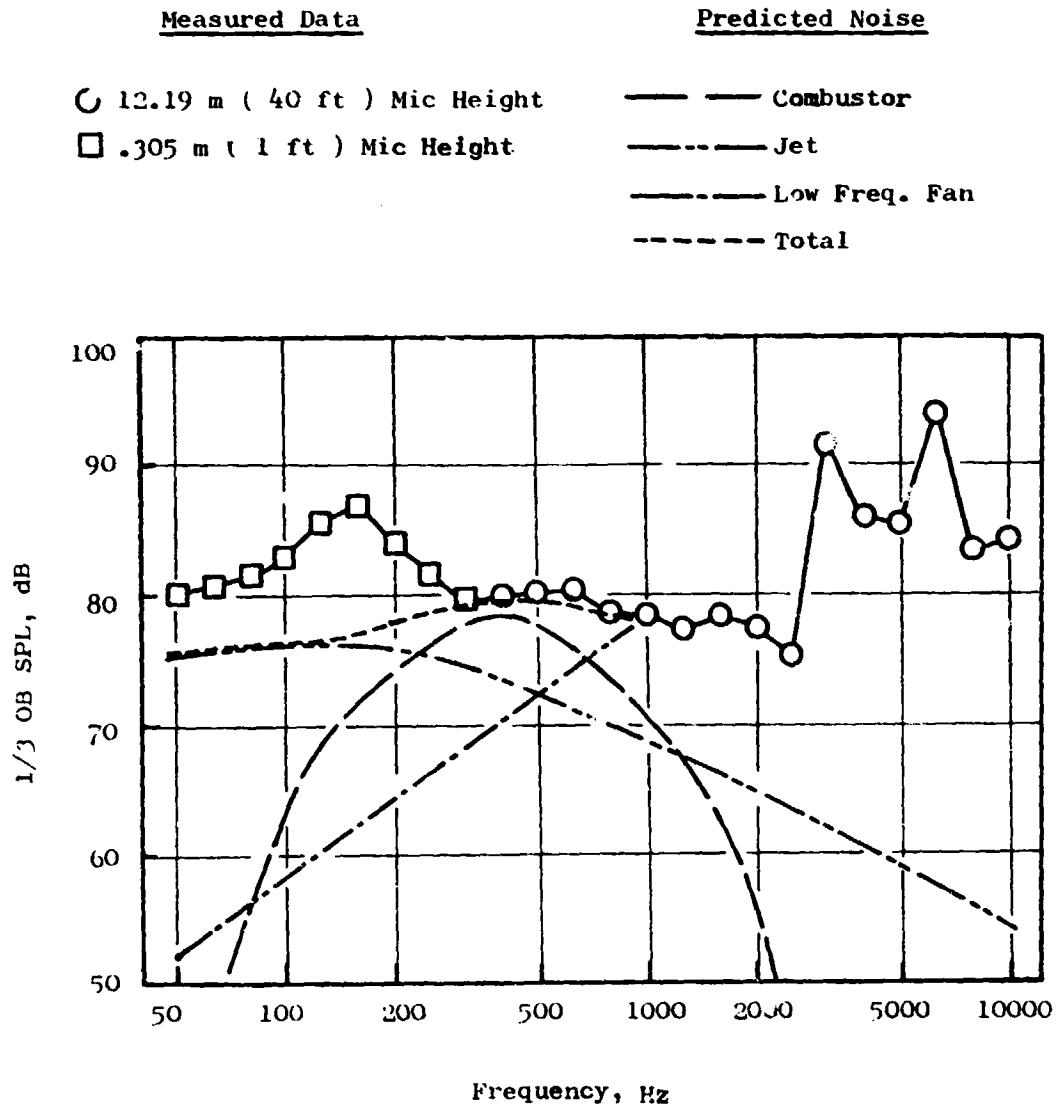


Figure 8. Comparison of Predicted and Measured Farfield Spectra, 54% Fan Speed.

- 120° acoustic Angle
- 67% Fan Speed
- 45.72 m (150 ft) Arc

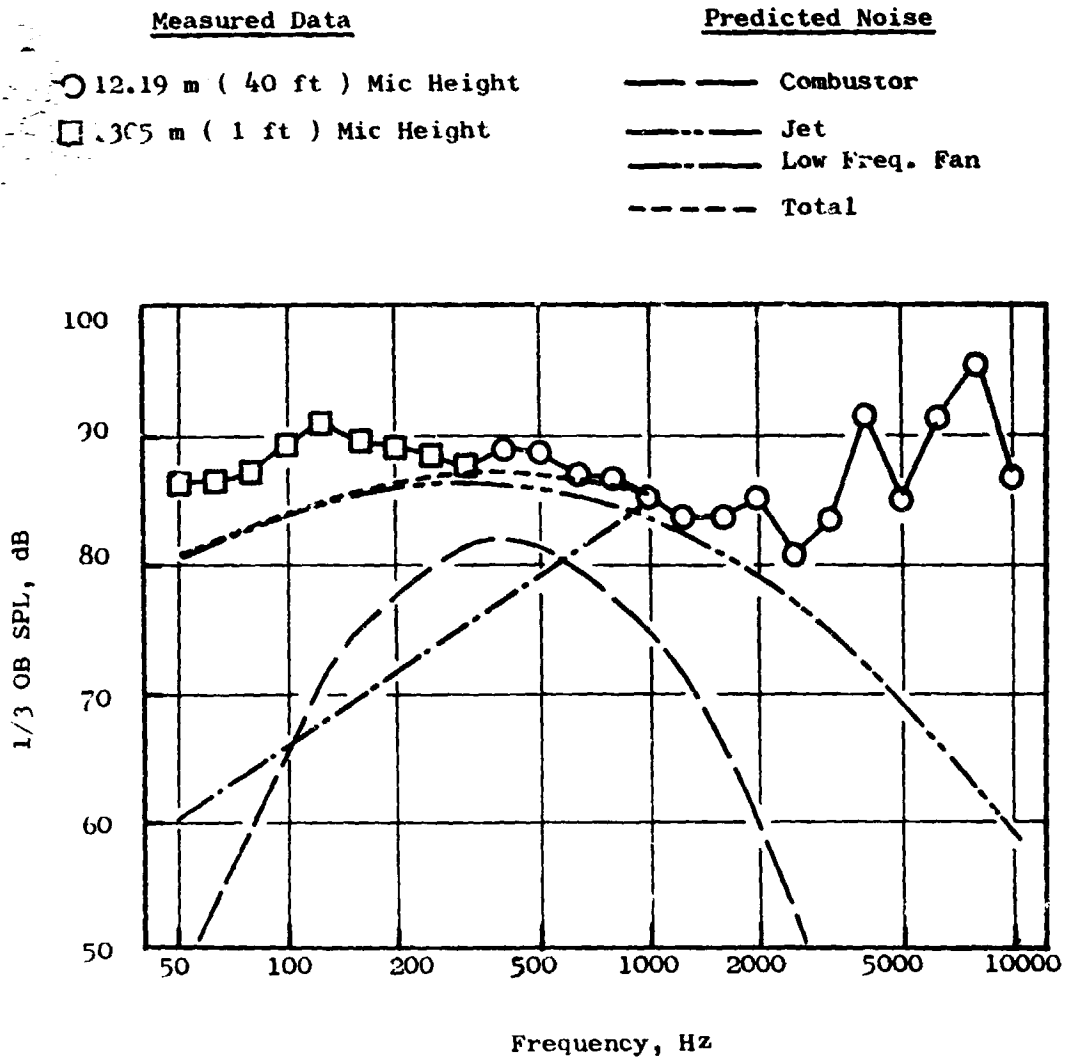


Figure 9. Comparison of Predicted and Measured Farfield Spectra, 67% Fan Speed.

- 120° Acoustic Angle
- 80% Fan Speed
- 45.72 m (150 ft) Arc

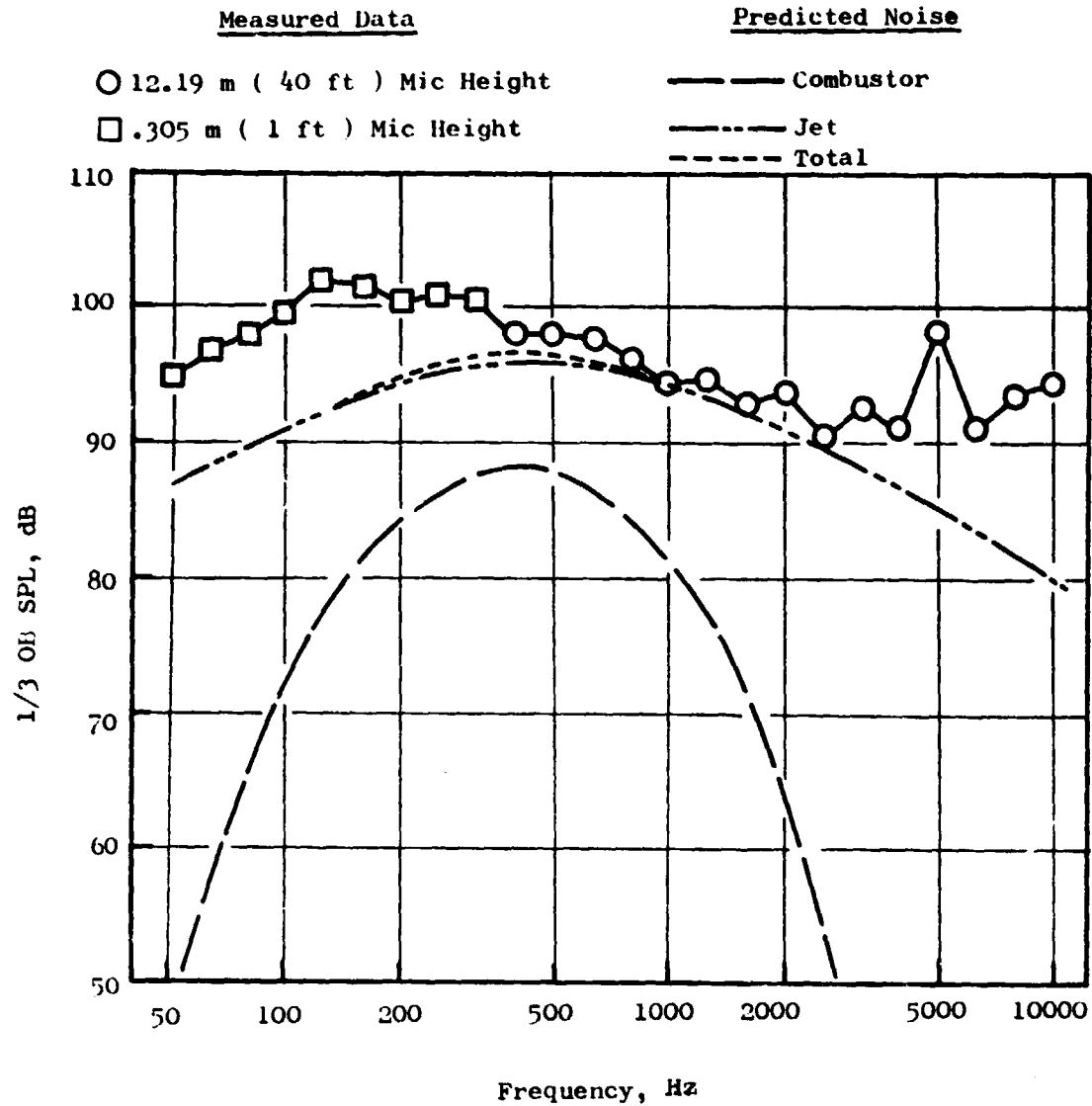


Figure 10. Comparison of Predicted and Measured Farfield Spectra, 80% Fan Speed.

- 120° Acoustic Angle
- 93% Fan Speed
- 45.72 m (150 ft) Arc

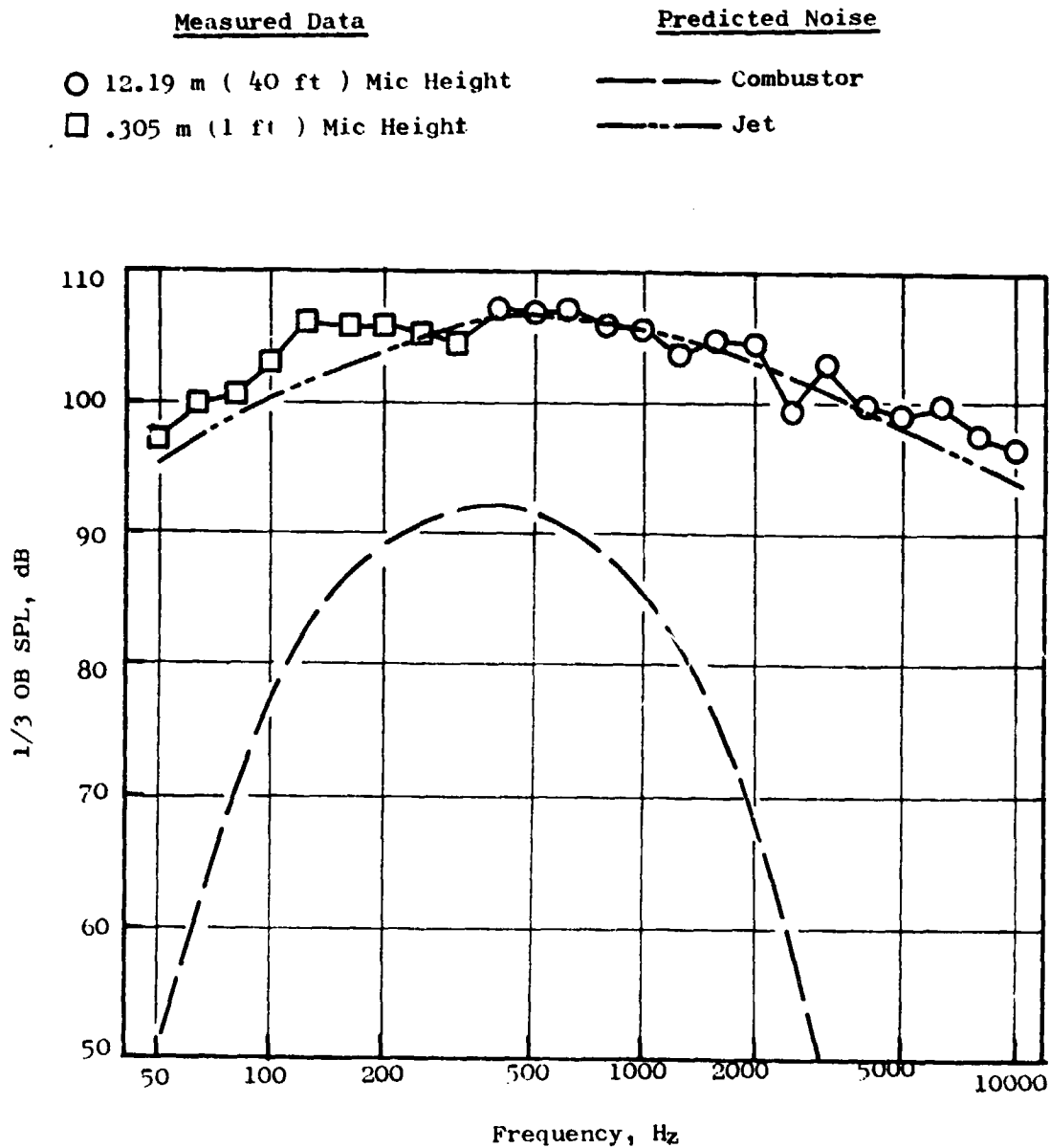


Figure 11. Comparison of Predicted and Measured Farfield Spectra, 93% Fan Speed.

The primary message to be gained from these comparisons is that the entire measured noise spectrum can be accounted for by means of the present noise prediction methods, with the exception of the 100 to 200 Hz region which is dominated by the combination of a core one-per-rev and an undefined source in the 110 to 130 Hz region. For low frequency combustion noise, the region from 200 to 400 Hz is of primary concern, and here the agreement is good. The two highest power settings (Figures 10 and 11) are, not unexpectedly, heavily jet-noise dominated. Some fan noise is still evident in the higher frequency bands. It is uncertain whether the 1000 Hz band SPL's are fan-dominated for these speeds; therefore no attempt was made to estimate the low frequency fan noise by ramping off from 1000 Hz as was done at the lower power settings. However, if the low-frequency fan noise estimated for the three lower power settings is extrapolated to the higher fan speeds, it can be seen that the fan and jet will account for the measured noise levels. The low frequency noise levels between 50 Hz and 100 Hz are higher than the predicted noise for several speeds. These levels were obtained from the 0.305 m (1 ft) microphones and corrected by 2 dB reduction. The correction could be as high as 6 dB for pressure doubling, that is no loss in amplitude for the reflected wave, however, this probably is not the case. A more realistic reason is a poor low frequency jet noise prediction.

The main area of interest in this test was, of course, in the lower power settings where combustor noise would be predicted to influence the low-frequency farfield noise. The fan speed at 67% is just sufficiently low for the combustor to have a noticeable effect on the farfield levels. Reference to Figure 9 shows that the measured levels in the 200 Hz to 500 Hz range are approximately 2 dB higher than the total of the predicted jet and estimated fan noise. The predicted combustor noise levels make up for some, but not all, of this difference. This is still in the region where the predicted jet noise dominates, so most of this difference could most logically be attributed to slight inaccuracies in the jet noise prediction. At the two lowest power settings, the combustor is predicted to dominate the aft angles in the 200 Hz to 630 Hz region, and the good agreement between measured and predicted levels is apparent. At the 41% fan speed (Figure 7), the differences between measured and predicted levels in the 50 Hz to 80 Hz region may again be due to the jet noise; the exit velocity for this fan speed is only 65.5 m/sec (215 ft/sec), and it was necessary to extrapolate the scale model jet data over a large range to reach this extremely low velocity. The possibility of course exists that extraneous noise sources, such as noise associated with flow off of the nozzle lip, may be entering the picture at these low power settings. The effect of the core engine one-per-rev is apparent at all lower speed points.

In order to aid in the determination of the dominant low-frequency far-field noise sources, examinations were made of the levels recorded in the 400 and 630 Hz bands. These bands are apparently free of the influence of ground effects and of the core one-per-rev tone, and are in the region of frequencies where the combustor noise is predicted to peak. For each frequency band, the measured farfield SPL at 120° was plotted logarithmically as a function of the jet velocity. A set of directivity plots was also made, by plotting the level recorded in each of the bands as a function of acoustic

angle, for each speed point. In each case the predicted component levels were also included for comparative purposes; the resulting diagnostic plots are shown on Figures 12 through 23. It should be noted here that the predicted jet noise as a function of the log of the jet velocity will not follow the straight-line, " V^x " relationship normally associated with this type of plot. The variable area nozzle opens up as the speed falls off, and the prediction is not normalized for this area change. Further, the jet spectrum peak frequency shifts to a higher value as the velocity increases. The result is a nonlinear relationship, especially for the lower frequency bands.

The data shows that a remarkably good correlation was achieved between measured and predicted levels at all speeds, for the predicted peak combustor noise angle. The directivity plots show that the correlation is not as good at the angles aft of this peak, but this appears to be due to underprediction of the jet noise at these angles. Examination of the directivities recorded at the higher speeds, which are clearly jet noise dominated, show that the jet noise prediction method seems to fall off too rapidly in the aft angles.

In summary, the farfield data show good correlation with the combustor noise prediction at the combinations of power setting, acoustic angle, and frequency band where combustor noise is expected to predominate. There are some instances where there are discrepancies between the measured levels and the summation of the predicted component levels, but in these cases, the measured directivities would indicate that sources other than combustor noise would be the more logical source of these discrepancies.

B. Acoustic Probe Data

As in the case of the farfield data, the data recorded from the core exhaust acoustic probe were reduced to one-third octave band SPL spectra. The SPL spectra from each of the five probe immersions were then integrated to obtain the measured PWL spectra in the core exhaust duct. The PWL spectrum thus recorded for each power setting is compared to the predicted combustor and turbine noise levels in Figures 24 through 28. It would at first appear from these comparisons that both the combustor and turbine noise predictions are on the order of 10-15 dB too low. As previously, discussed, the waveguide probe records aerodynamic turbulence as well as "real" noise levels. This problem might account for some of the difference, but it can also be seen that there are apparent discrepancies between predicted and measured pure tone levels. The tone PWL's recorded on probes usually are accurate, so there must be some other source of error. The prediction procedures used for the turbine and combustor, it should be remembered, are semi-empirical correlations based on farfield noise measurements. The predicted PWL spectra thus shown on the figures are actually "farfield PWL's", not in-duct values; the effects of any duct transmission and radiation phenomena are not accounted for. However, the magnitude of the observed differences between prediction and measurement still seems rather large to attribute only to duct transmission effects.

- 120° Acoustic Angle
- 400 Hz
- 45.72 m (150 ft) Arc

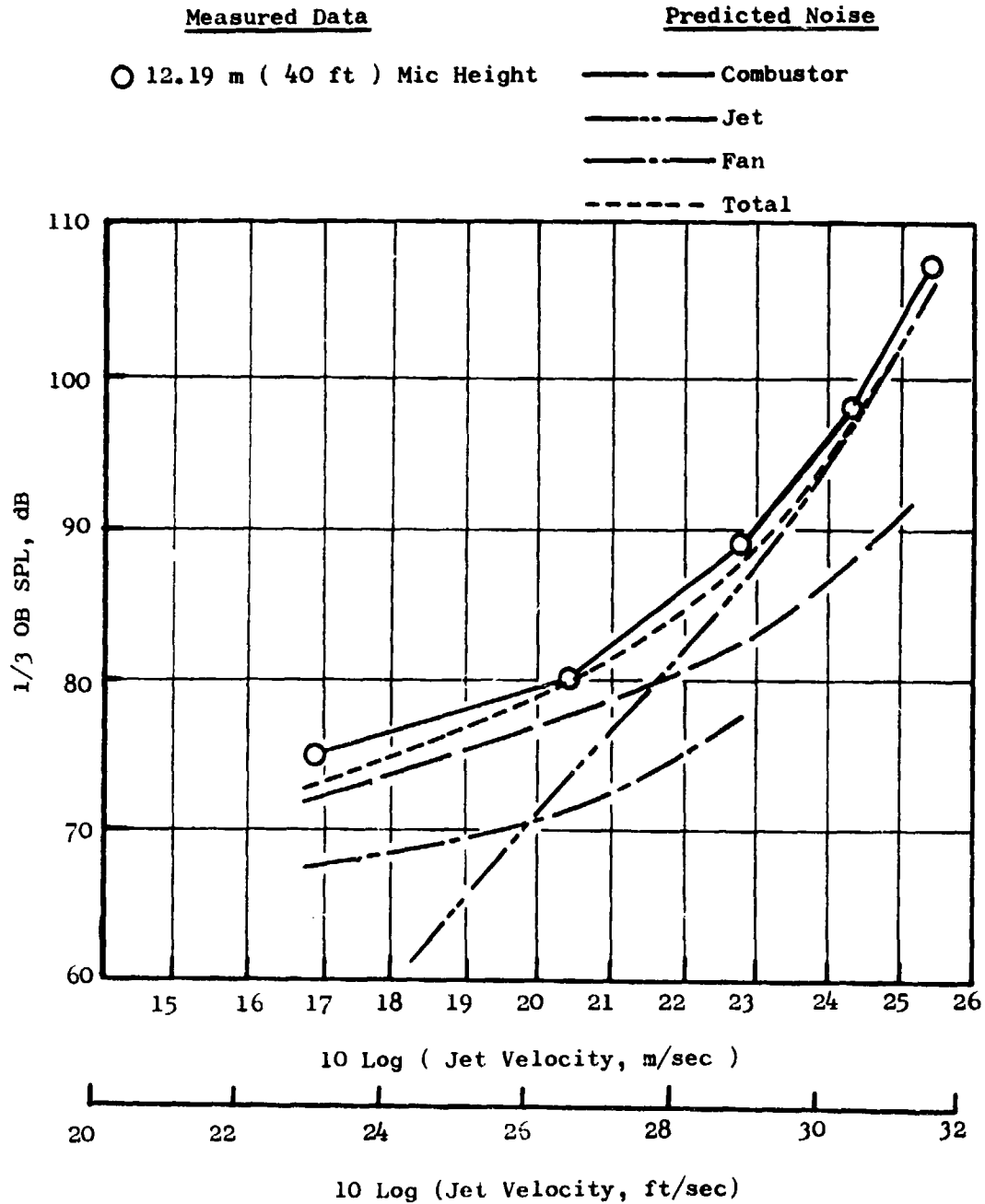


Figure 12. 400 Hz 1/3-Octave Band SPL Versus Jet Velocity.

- 65.5 m/ sec (215 ft/sec) Jet Velocity
- 400 Hz
- 45.72 m (150 ft) Arc

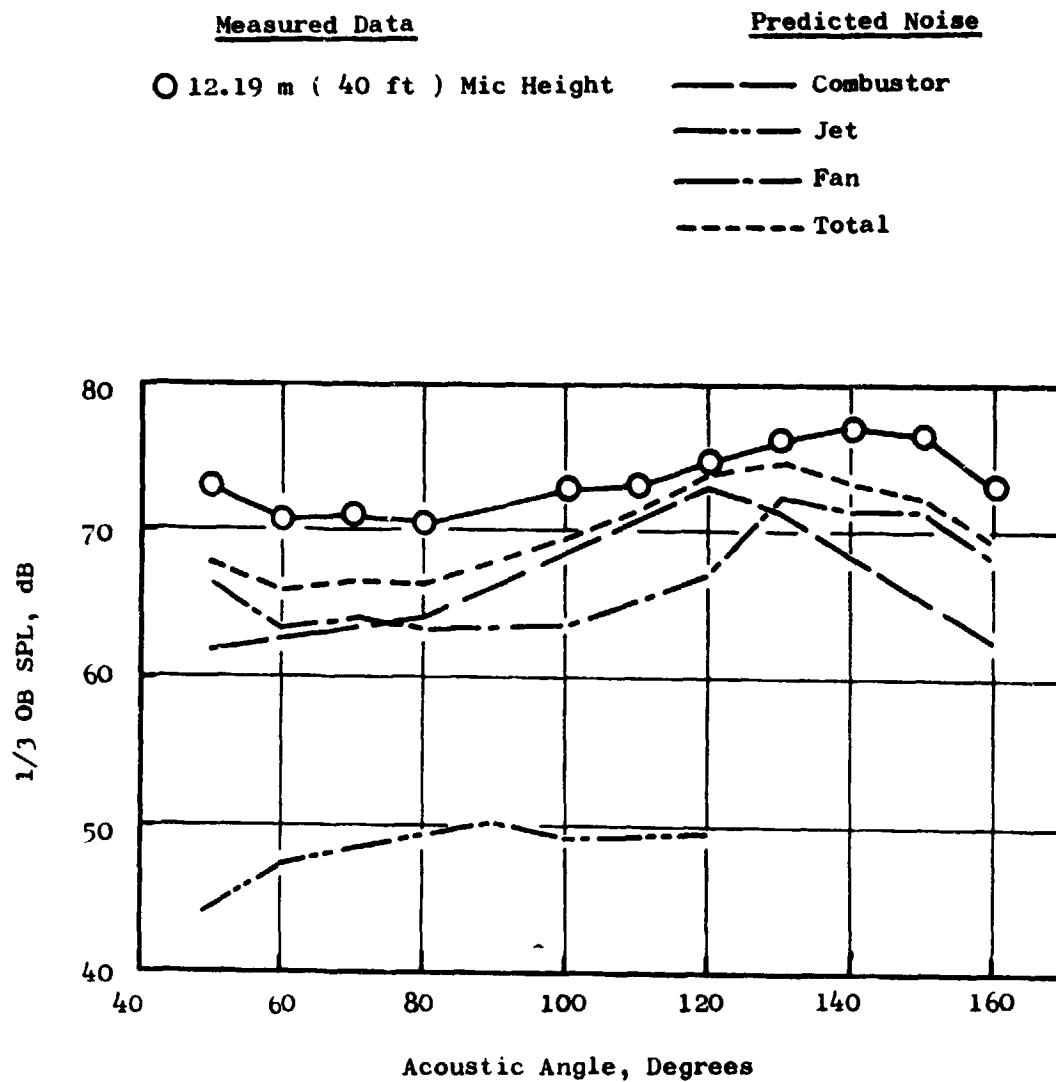


Figure 13. 400 Hz 1/3-Octave Band SPL Directivity, 41% Fan Speed.

- 138.7 m/sec (455 ft/sec) Jet Velocity
- 400 Hz
- 45.72 m (500 ft) Arc

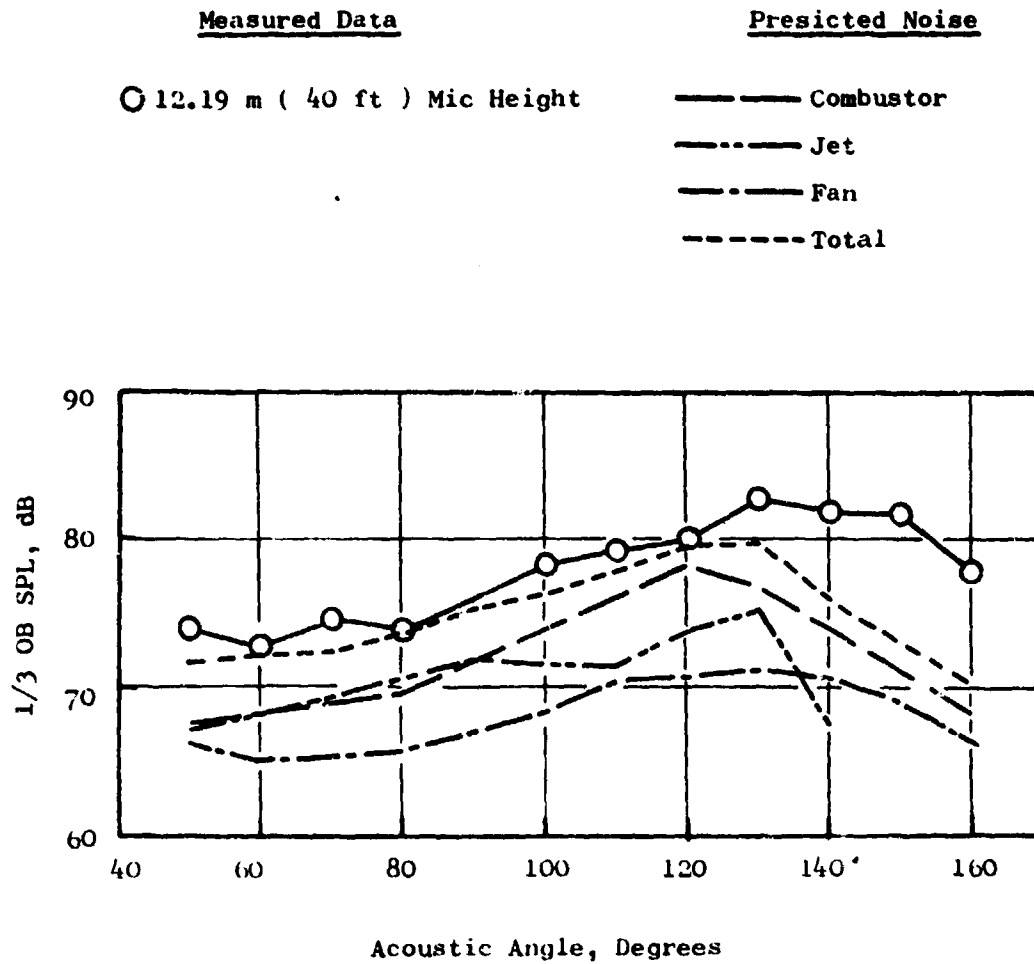


Figure 14. 400 Hz 1/3-Octave Band SPL Directivity, 54% Fan Speed.

- 234.7 m/sec (770 ft/sec) Jet Velocity
- 400 Hz
- 45.72 m (150 ft) Arc

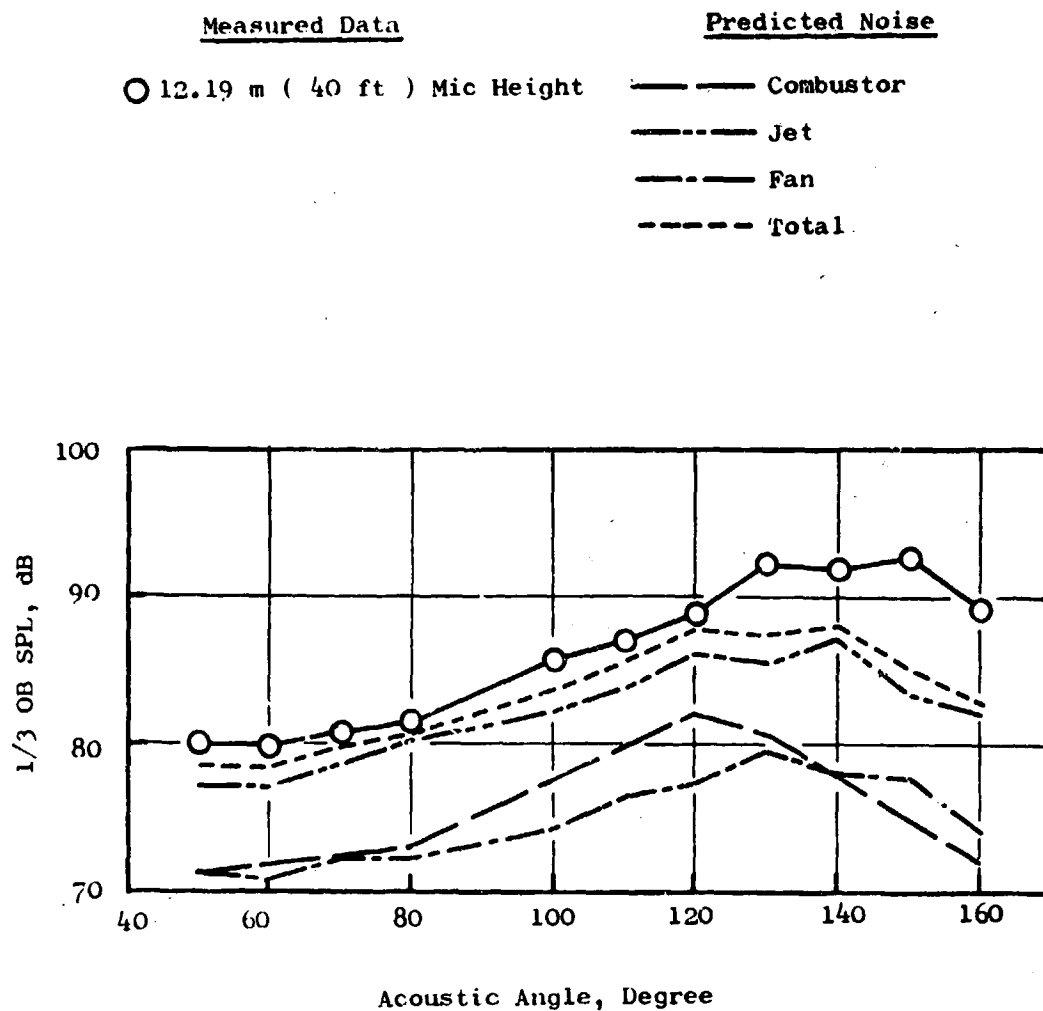


Figure 15. 400 Hz 1/3-Octave Band SPL Directivity, 67% Fan Speed.

- 445 m/sec (1460 ft/sec) Jet Velocity
- 400 Hz
- 45.72 m (150 ft) Arc

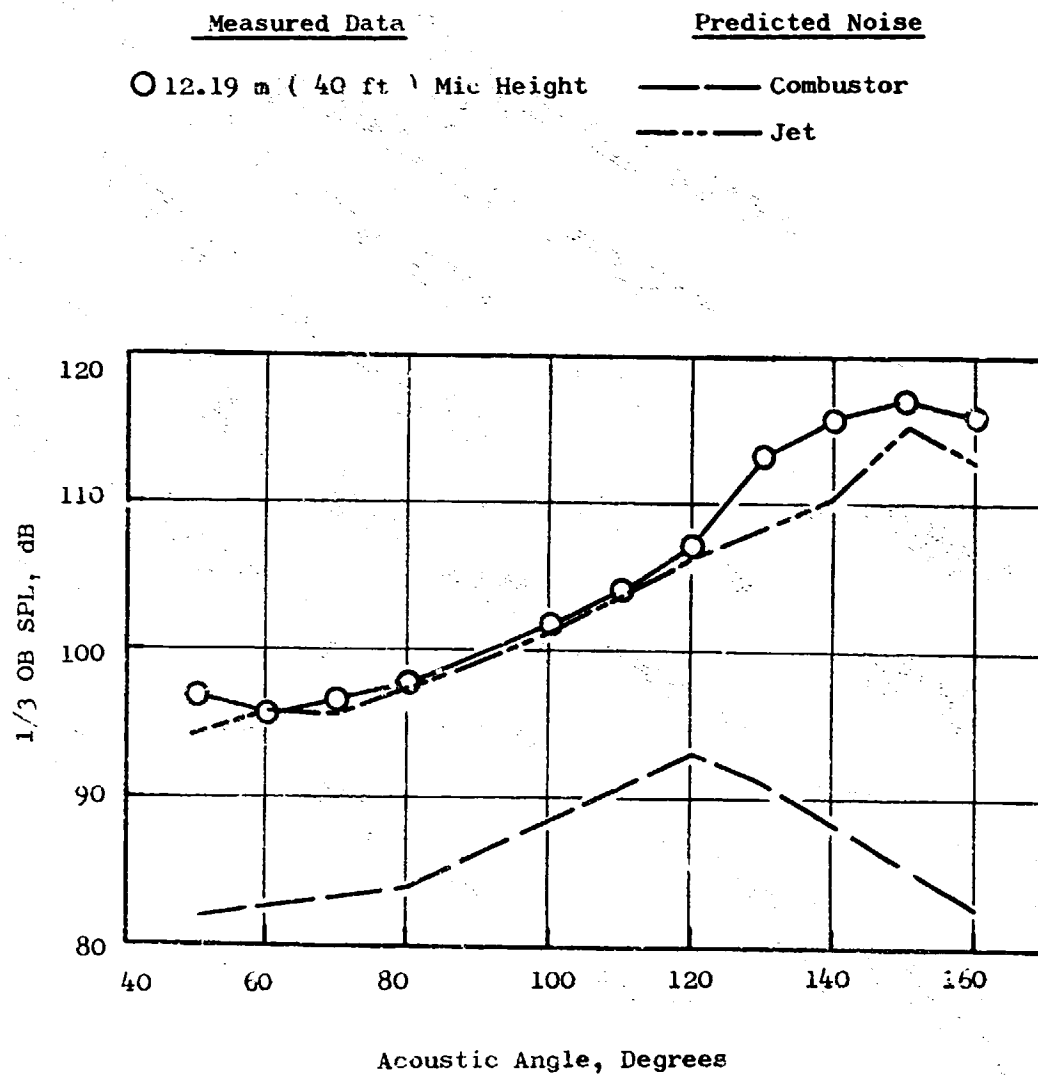


Figure 17. 400 Hz 1/3-Octave Band SPL Directivity, 93% Fan Speed.

- 120° Acoustic Angle
- 630 Hz
- 45.72 m (150 ft) Arc

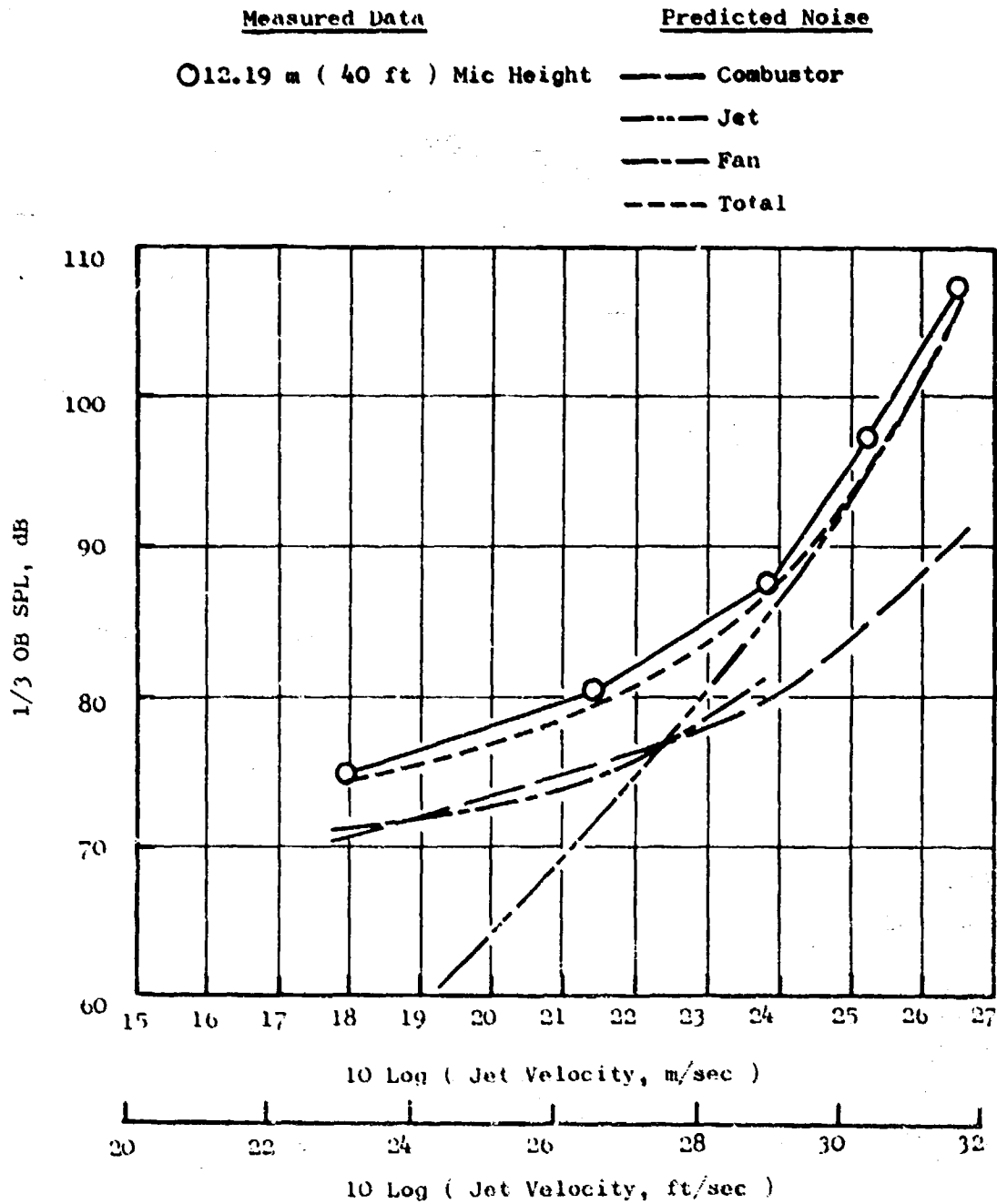


Figure 18. 630 Hz 1/3-Octave Band SPL Versus Jet Velocity.

- 138.7 m/sec (455 ft/sec) Jet Velocity
- 630 Hz
- 45.72 m (150 ft) Arc

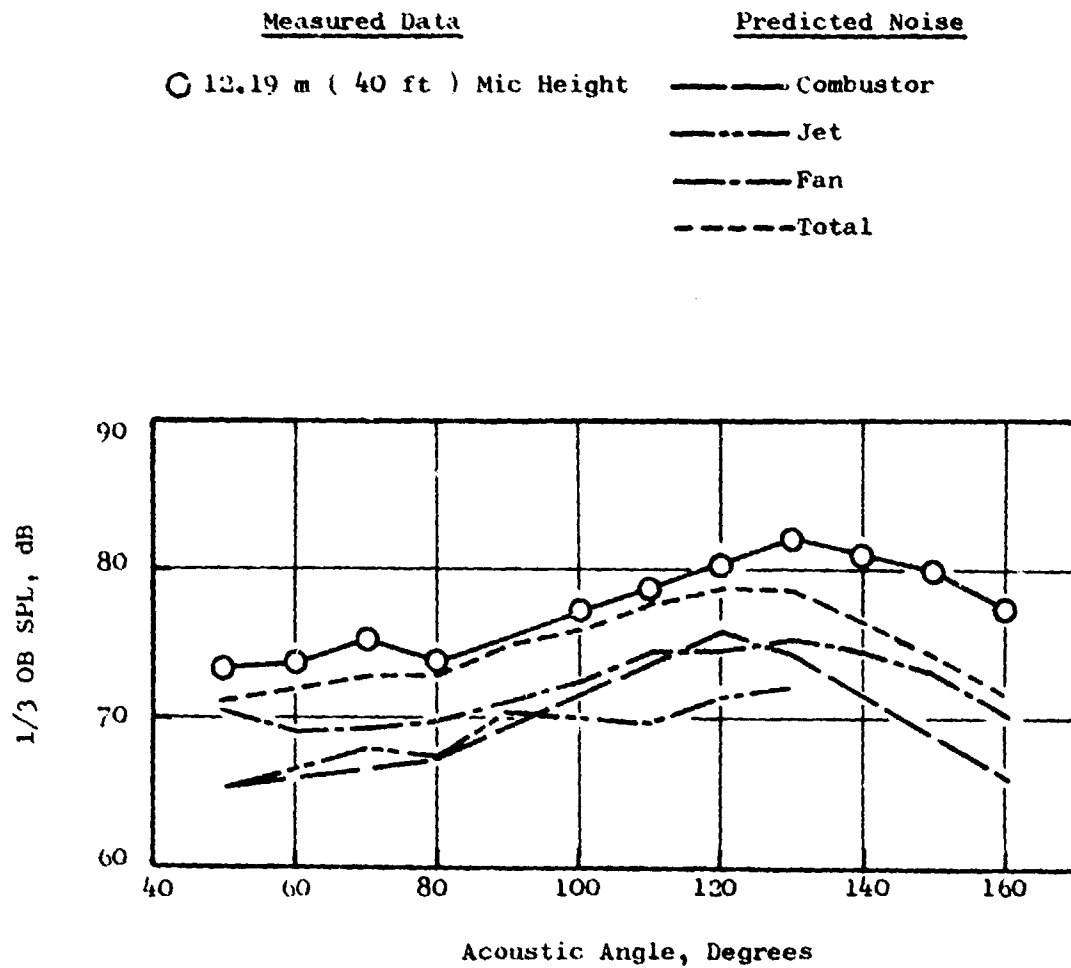
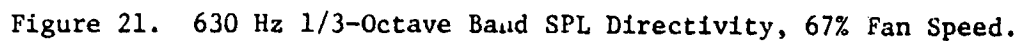
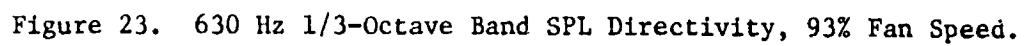


Figure 20. 630 Hz 1/3-Octave Band SPL Directivity, 54% Fan Speed.

- | <u>Measured Data</u> | <u>Predicted Noise</u> |
|--------------------------------|------------------------|
| ○ 12.19 m (40 ft) Mic Height | ————— Combustor |
| | ——— Jet |
| | ————— Fan |
| | ----- Total |



- Measured Data
- O 12.19 m (40 ft) Mic Height
- Predicted Noise
- Combustor
- Jet



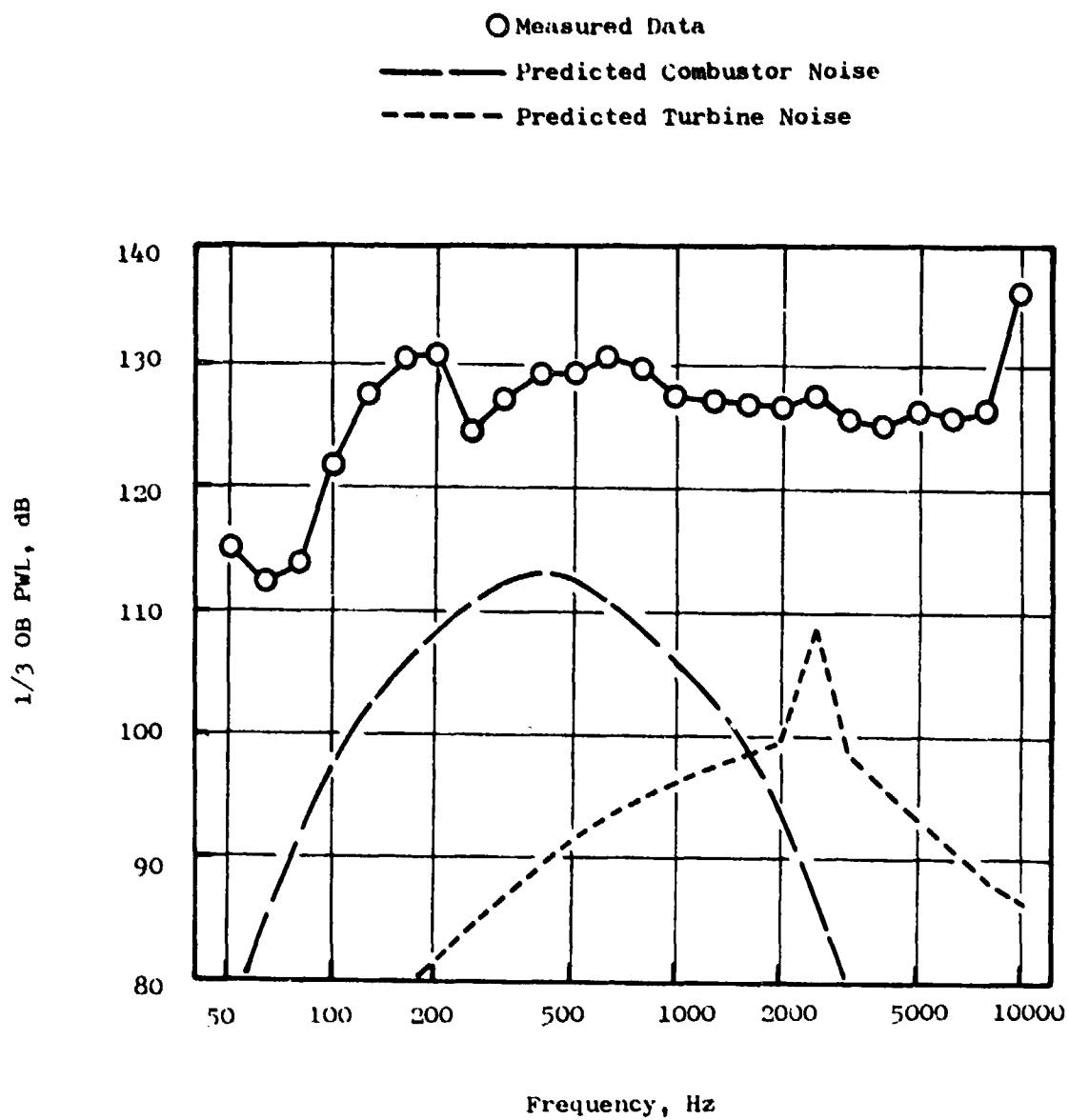


Figure 24. Core Probe PWL Spectrum, 22% Fan Speed.

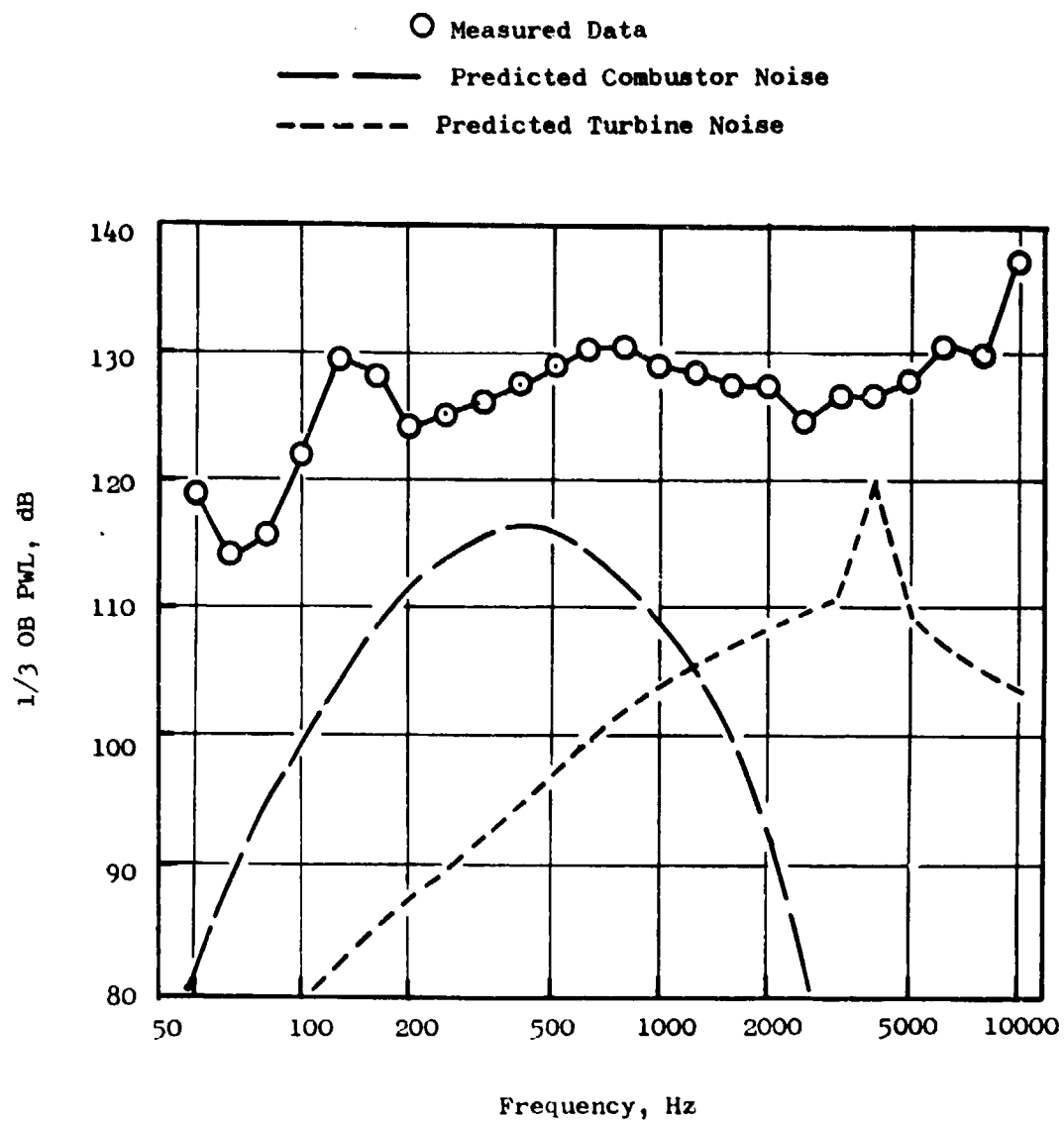


Figure 25. Core Probe PWL Spectrum, 32% Fan Speed.

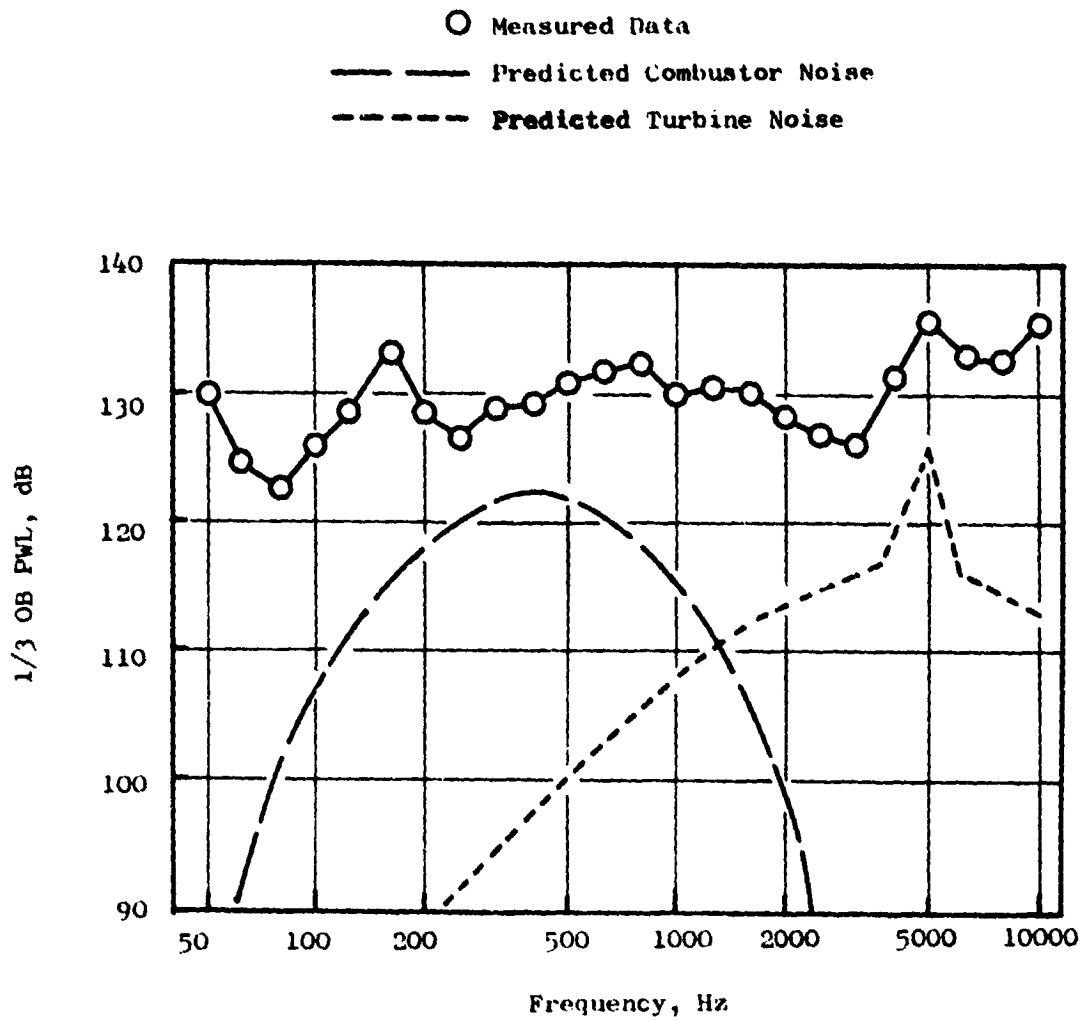


Figure 26. Core Probe PWL Spectrum, 41% Fan Speed.

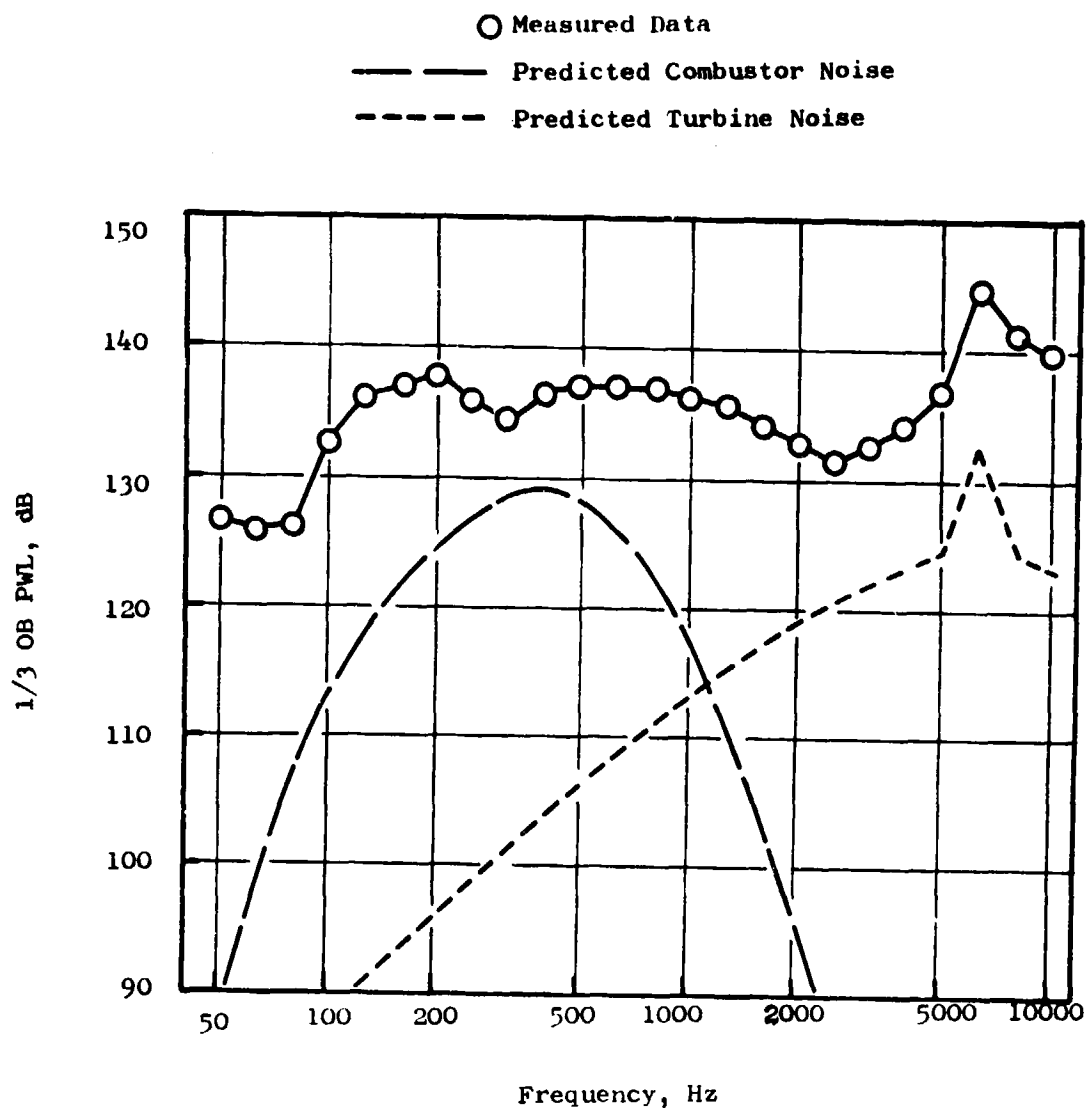


Figure 27. Core Probe PWL Spectrum, 53% Fan Speed.

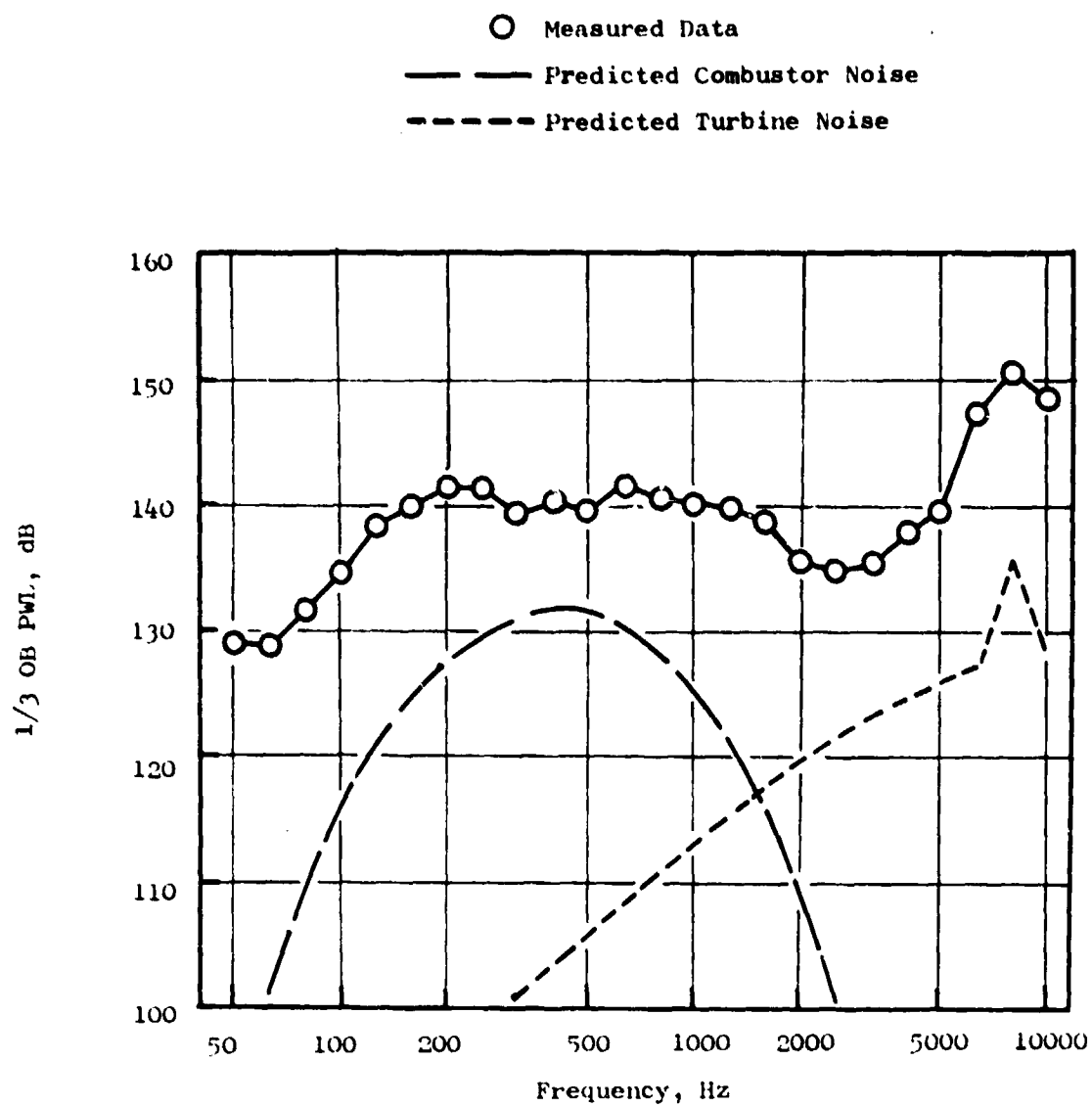


Figure 28. Core Probe PWL Spectrum, 64% Fan Speed.

In order to investigate the noise sources in more detail, the data were reduced to 20 Hz narrowband SPL spectra for each immersion. Figures 29 through 33 are typical representations of these spectra; the levels recorded for the immersion in the center of the duct (Immersion No. 3) are presented for each of the five power settings. In each case, the identifiable pure tones are labeled as to their source. It may be seen that the strongest contributor to the recorded pure tone noise level is, surprisingly, the fan exhaust noise. The blade passing fundamental tone for the second stage of the fan lies in the same one-third octave band as does the fundamental tone for the second stage of the low pressure turbine (the LPT second stage is the predicted "dominant" noise source for turbine noise). It is further evident, from the narrowband spectra, that the fan tone levels in the core duct are in most cases higher than the turbine tone levels. The recorded pure tone PWL in the one-third octave band spectral plots shown in Figures 24 through 28 is thus seen to be mostly due to the fan. Even if the fan tone were "removed", the remaining LP turbine stage two fundamental tone would still be masked out by the broadband noise when the levels were summed up on a one-third octave band basis, and no strong turbine tone would be evident in the spectrum.

This apparent domination of the core duct high frequency noise by the fan is perhaps not too surprising when we consider the high noise level exhibited by the unsuppressed fan in the farfield. Also, it must be remembered that the core probe stem extends across the full width of the fan duct in order to reach into the core duct; thus approximately 20.3 cm (8 in.) of the stem is exposed to the high fan noise levels. Past experience with waveguide probes has shown that they will transmit structure-borne vibrations to the microphone, and this could be occurring here.

The narrowbands thus provide a good case for attributing the differences between measurement and prediction to fan noise "contamination", for the high frequency bands; however, they provide no conclusions regarding the discrepancies observed at low frequencies. These low frequency differences are particularly puzzling, since the farfield data indicates that the combustor noise predictions are reasonable. Consideration of the most likely reasons for the low frequency discrepancies leads to two possibilities: (1) The combustor noise levels in the duct are actually higher than the prediction, even though there is good agreement in the farfield; such a difference could be due to neglecting duct transmission characteristics, as has already been suggested, or, (2) the measured low frequency signals are actually flow-related aerodynamic fluctuations in the core duct, another previously-discussed possibility.

As was done for the farfield data, a "diagnostic" plot was made in an attempt to determine the source of the measured low frequency noise. Figure 34 is a plot of the measured one-third octave band PWL recorded on the probe for the 80 Hz, 250 Hz, 400 Hz, 630 Hz, and 1000 Hz bands. The data are plotted as a function of 20 times the logarithm of the factor "K" and normalized to the PWL at a value of 80. K is the correlating factor for the combustor noise prediction, and is defined as:

• 20 Hz Bandwidth

• Immersion No. 3

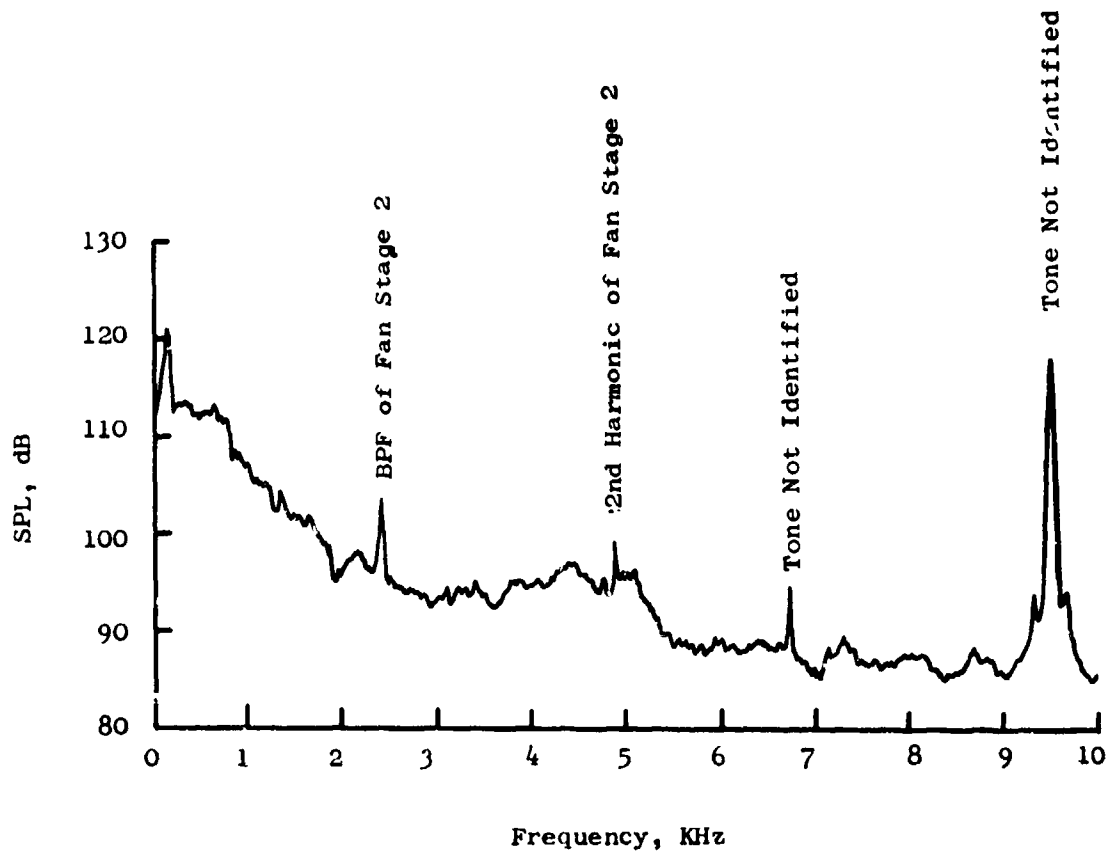


Figure 29. Core Probe Narrowband SPL Spectrum, 22% Fan Speed.

• 20 Hz Bandwidth

• Immersion No. 3

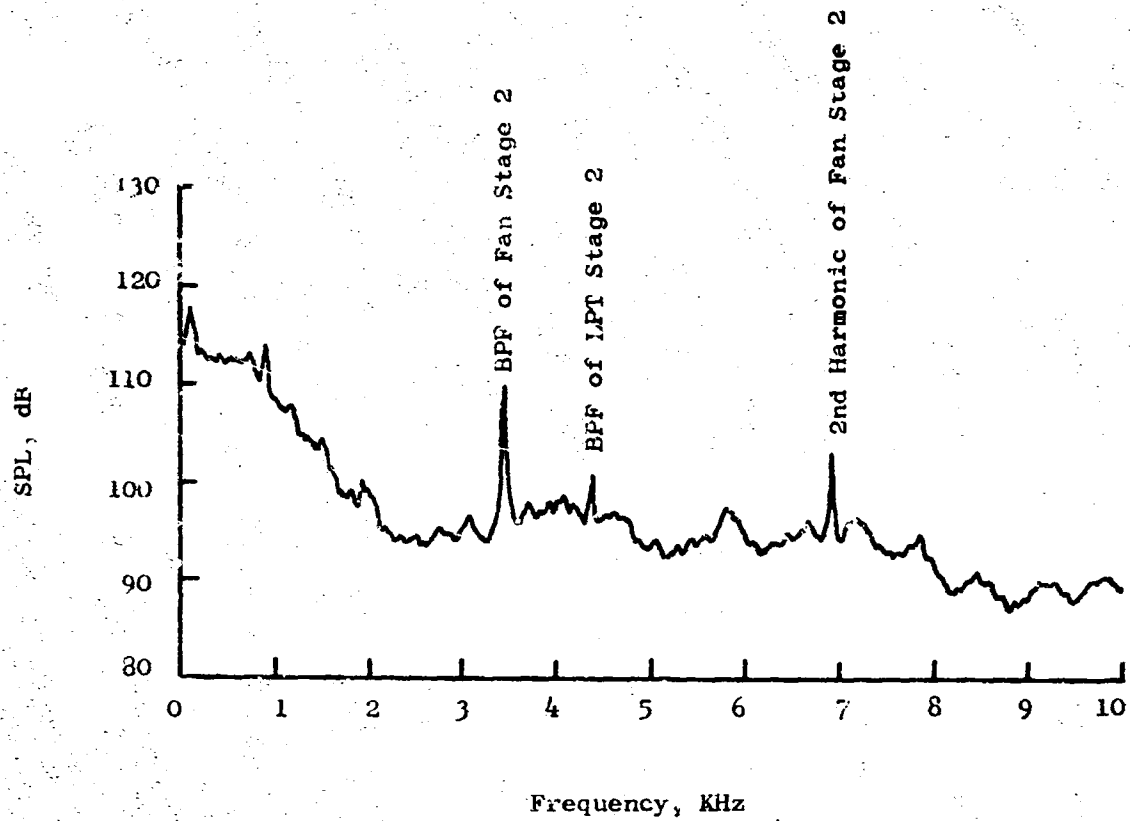


Figure 30. Core Probe Narrowband SPL Spectrum, 32% Fan Speed.

• 20 Hz Bandwidth

• Immersion No. 3

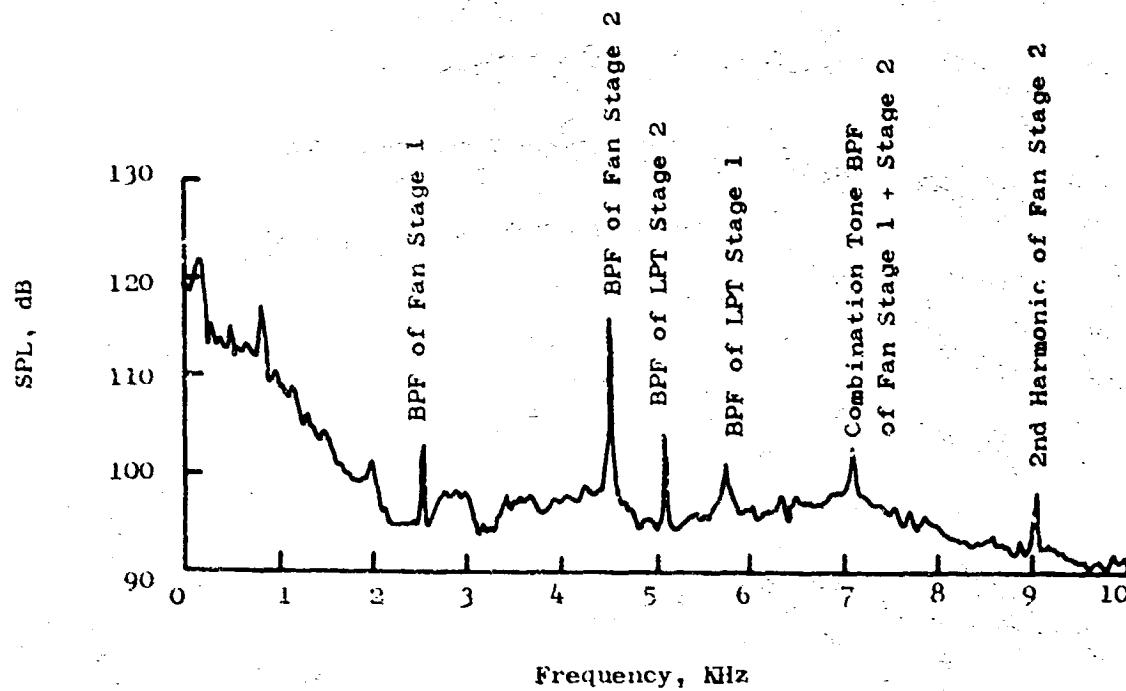


Figure 31. Core Probe Narrowband SPL Spectrum, 41% Fan Speed.

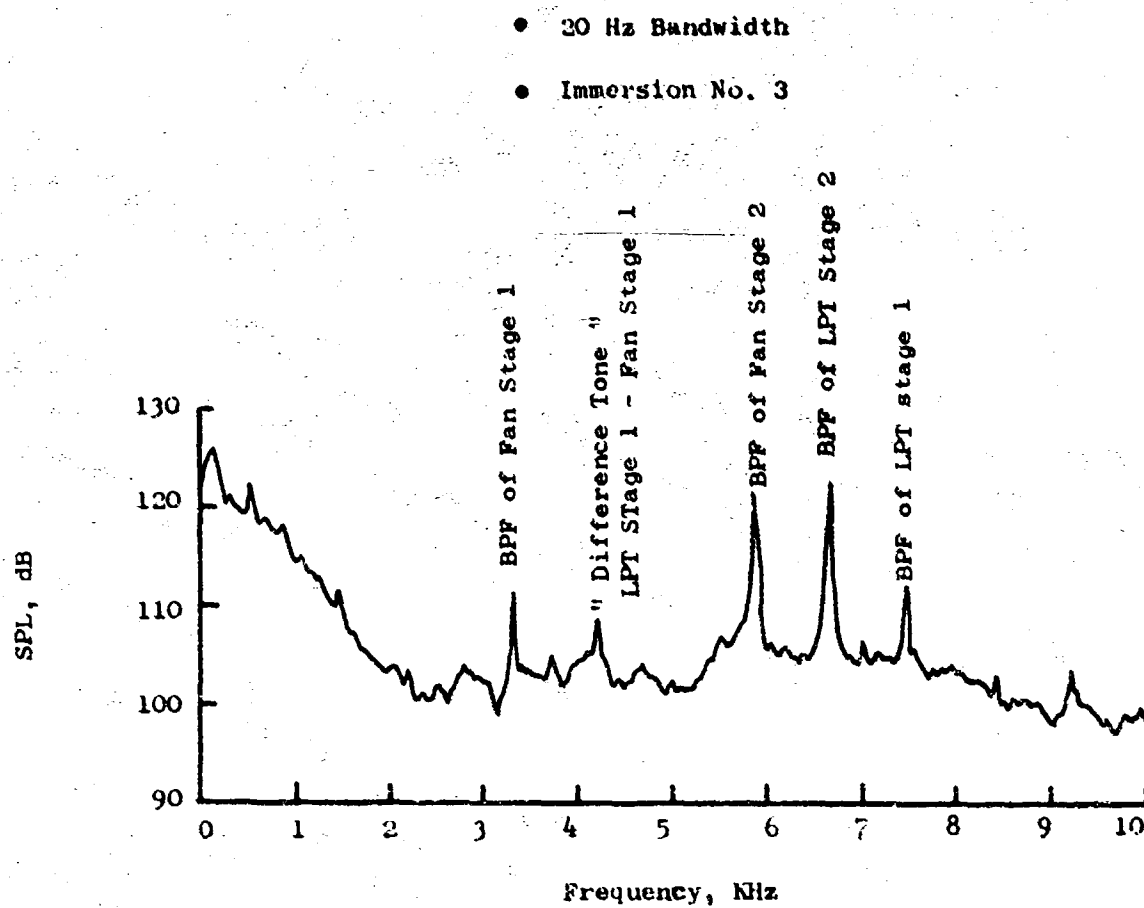


Figure 32. Core Probe Narrowband SPL Spectrum, 53% Fan Speed.

• 20 Hz Bandwidth

• Immersion No. 3

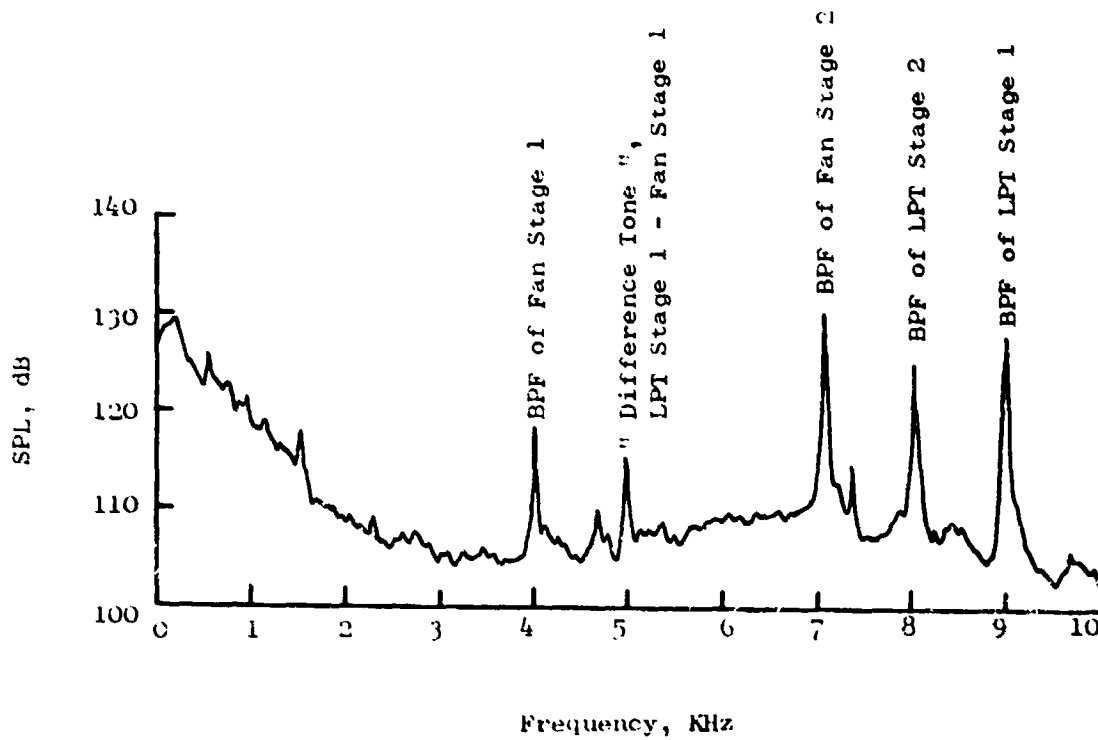


Figure 33. Core Probe Narrowband SPL Spectrum, 64% Fan Speed.

$$\bullet K = (T_4 - T_3) \sqrt{W_3} (P_3/P_0) (T_0/T_3)$$

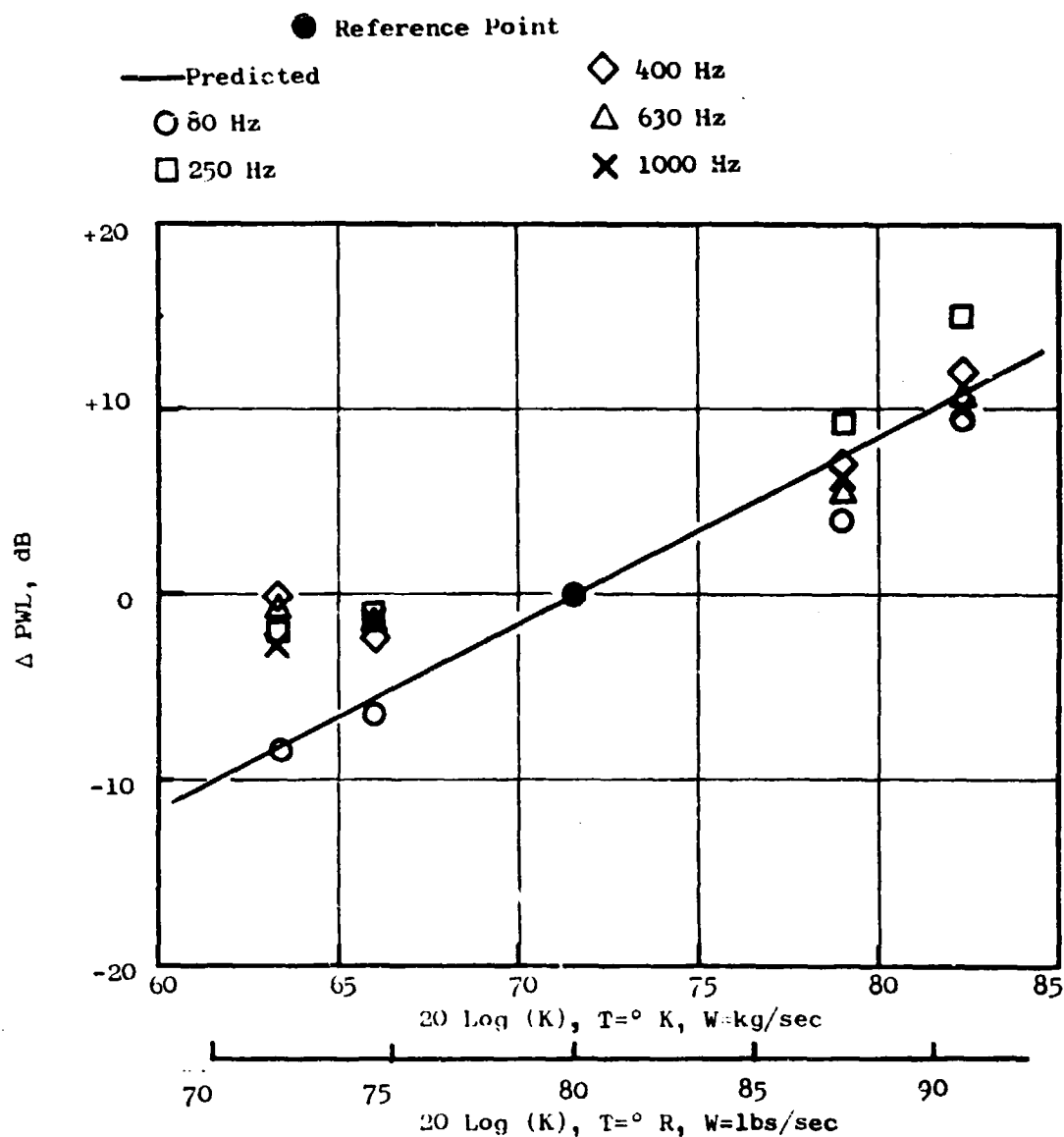


Figure 34. Probe Measured 1/3-Octave Band PWL Versus 20 log (K).

$$K = (T_4 - T_3) \sqrt{w_3} \frac{P_3}{P_0} \frac{T_0}{T_3}$$

wherein the subscript 3 denotes the combustor inlet conditions, 4 the combustor exit, and 0 the ambient value. The predicted levels, based on observed combustor noise data, follow a linear relationship with $20 \log K$. It may be seen from this plot that the probe-recorded levels do not follow the same slope as the predictions. The measured data thus differs from the predicted combustor noise predictions in behavior as well as in absolute level.

The only parts of the measured probe data that thus can be definitely attributed to the core are the turbine pure tone levels. As already noted, the fundamental tone from the second stage of the low pressure turbine is the predicted dominant tone for turbine noise measured in the farfield. This tone is evident in all of the narrowband plots, save for the very lowest speed point. The total PWL for this tone was obtained by integrating the measured tone SPL's across the duct area. This was done at each speed point. The resulting values are compared to the predicted pure tone PWL's, as a function of turbine pressure ratio, in Figure 35. The measured tone levels are within 2-3 dB of the predicted values at the two lower turbine pressure ratios, but at the higher pressure ratios they are 5-10 dB higher than predicted. Once again, it must be remembered that the turbine noise prediction employed is based on farfield data correlations, and that comparisons with duct data thus are based on the assumption that any "in-duct" phenomena are negligible. The final report from the Core Engine Noise Program (Reference 1) contains data from various engines in support of the turbine noise prediction. In these cases, the farfield tone PWL's agree quite well with the predicted values, but the corresponding tone PWL's measured in the duct exhibit the same behavior as shown in Figure 35. It was speculated in the referenced report that duct resonances are responsible for the apparently erratic behavior of the probe-measured turbine tone levels in regard to the predicted values. It may be that the same phenomena are occurring for the F101, but there are unfortunately no farfield turbine noise measurements available to confirm this.

The analysis of the core probe data thus indicates that the recorded noise levels are possibly influenced by extraneous signals. The combustor broadband predicted duct noise levels do not account for the recorded probe levels, but there is fairly good agreement in the farfield. The turbine pure tone PWLs are also higher than predicted in some instances, but previous test data indicates that these differences may not be significant. It would appear, unfortunately, that no definite conclusions can be drawn from the probe data.

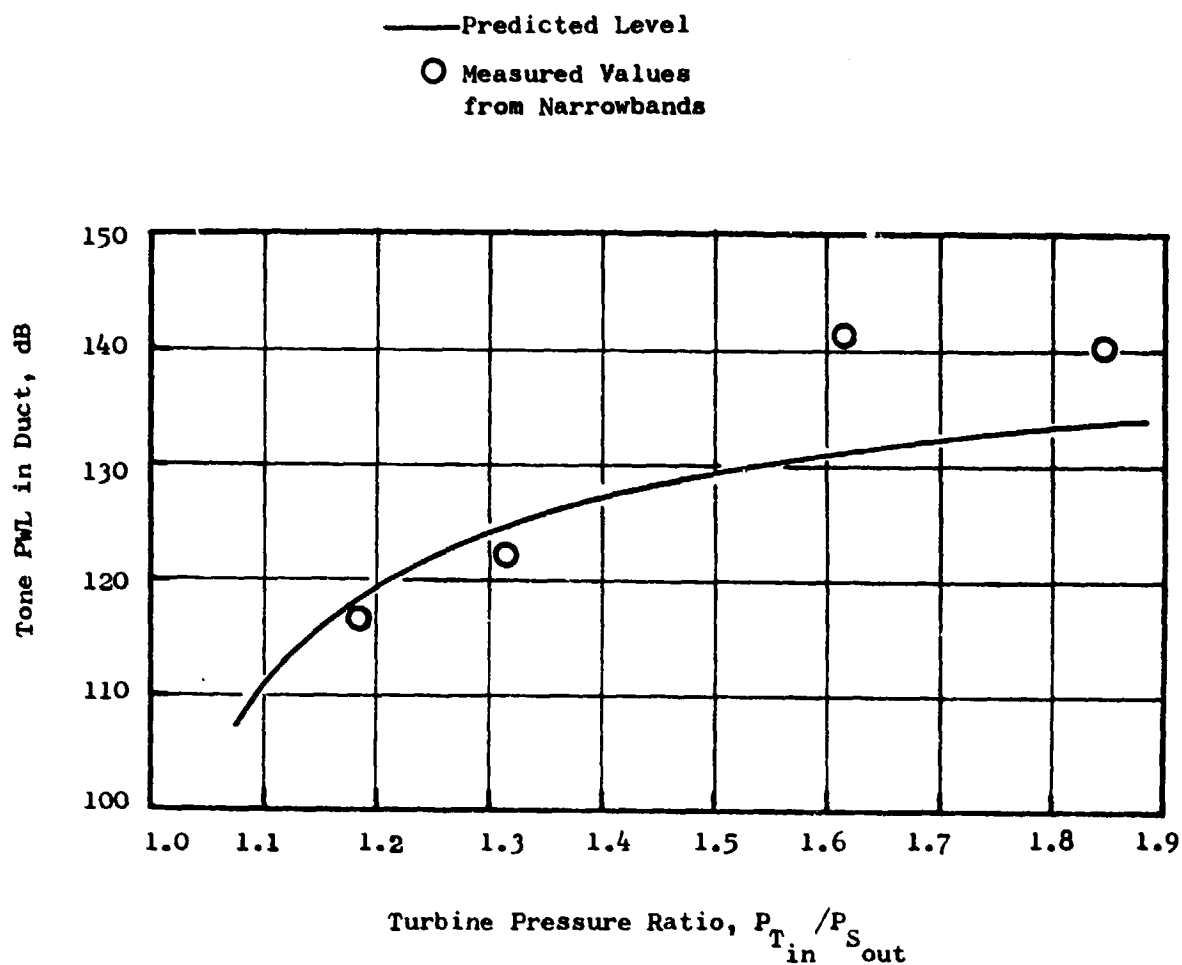


Figure 35. Low Pressure Turbine Stage 2 Fundamental PWL Versus Turbine Pressure Ratio.

SECTION V

CONCLUSIONS

The necessity of using only very low power settings in this test series means that the "direct" applicability of the data to the QCSEE engines is somewhat limited. Reference to the cycle data for both the QCSEE UTW and OTW engines indicates that the combustor and low pressure turbine operating conditions (at both approach and takeoff) are matched by the F101 test points only at fan speeds of 79% and above. At these speeds, the farfield data is totally dominated by jet and fan noise. The data were therefore used to determine the general applicability of the combustor and turbine noise prediction procedures to the F101 core engine employed for QCSEE.

The low frequency farfield core noise measurements support the QCSEE predictions. The high frequency core noise predictions, however, are unconfirmed by farfield data due to the masking of this noise by other sources. The probe data was inconclusive and contradictory to the farfield results. If it is assumed that the measured probe levels are correct, it would mean that the present QCSEE noise estimates are underpredicting the core noise in the duct. However, the system perceived noise levels are dependent on the noise radiated to the farfield. The fact that noise levels in the duct are underpredicted is of little importance, if the farfield levels are accurately estimated; this is apparently the case for the low frequency noise from the combustor. The discrepancies in high frequency broadband core noise cannot be dismissed as easily, since there is no uncontaminated farfield data to measure against. The present core acoustic suppressor design for the QCSEE engine has an inherently large margin of high frequency suppression, the levels being approximately twice as large as the preliminary predictions indicated to be necessary. If the unsuppressed high frequency core noise is truly greater than predicted in the farfield, it will be offset by this additional suppression.

Within the limited nature of this test data, it is concluded that there is no reason to modify the core internal noise predictions or core treatment design presently employed for the QCSEE engines.

SECTION VI

REFERENCE

1. Kazin, S.B., Matta, R.K., "Core Engine Noise Control Program, Volume III - Prediction Methods", General Electric Company DOT/FAA Report FAA-RD-74-125, III, August 1974.